Zeitschrift für Kristallographie, Bd. 139, S. 351—378 (1974)

The crystal structure of plagionite, $Pb_5Sb_8S_{17}$, the second member in the homologous series $Pb_{3+2n}Sb_8S_{15+2n}$

By SEUNG-AM CHO and B. J. WUENSCH

Ceramics Division, Department of Metallurgy and Materials Science
Massachusetts Institute of Technology, Cambridge, Massachusetts

Dedicated to Prof. M. J. Buerger on the occasion of his 70th birthday

(Received 18 August 1973)

Auszug

Plagionit $Pb_5Sb_8S_{17}$ hat die Raumgruppe $C2/c$, die Gitterkonstanten $a = 13{,}4857(8)$, $b = 11{,}8656(4)$, $c = 19{,}9834(7)$Å, $\beta = 107{,}168(4)°$; $Z = 4$, $D_{gem} = 5{,}54$ g cm^{-3}, $D_x = 5{,}55$ g cm^{-3}. Das Mineral gehört zur Serie der Homologen $Pb_{3+2n}Sb_8S_{15+2n}$, die im Gegensatz zu anderen Schwefelantimoniden tafeligen Habitus aufweisen. Die Struktur wurde mittels des Verfahrens der symbolischen Addition bestimmt und nach der Methode der kleinsten Quadrate bis zu $R = 18{,}2\%$ für 2302 beobachtbare Interferenzen verfeinert. Die asymmetrische Einheit enthält 16 Atome. Zwei Pb-Atome werden von sechs bzw. sieben S-Atomen in oktaeder-ähnlichen Koordinationen umgeben; ein drittes Pb-Atom hat eine unregelmäßige Umgebung aus acht S-Atomen. Drei der vier symmetrie-unabhängigen Sb-Atome sind von S-Atomen tetragonal-pyramidal, das vierte trigonal-pyramidal umgeben. Von den neun S-Atomen haben vier eine tetragonal-pyramidale Umgebung, drei eine verzerrt-tetraedrische und zwei eine dreizählige Koordination.

Die Plagionit-Struktur setzt sich aus Schichten einer PbS-ähnlichen Struktur zusammen, die sich durch die zweizählige b-Achse wiederholen, in der c-Richtung abwechselnd nach $(1\bar{1}2)$ und (112) gestapelt sind und sich unbegrenzt längs $[\bar{1}10]$ bzw. $[110]$ erstrecken. Es wird angenommen, daß die Strukturen der anderen Mitglieder der Serie ähnliche Schichten aufweisen, die sich durch die Breite der PbS-ähnlichen Bereiche unterscheiden.

Abstract

Plagionite, $Pb_5Sb_8S_{17}$, is monoclinic, space group $C2/c$, with $a = 13.4857(8)$, $b = 11.8656(4)$, $c = 19.9834(7)$ Å, $\beta = 107.168(4)°$, $\varrho_{meas} = 5.54$ g cm^{-3} and $\varrho_{cal} = 5.55$ g cm^{-3} for $Z = 4$. The mineral is the second member of an homologous series $Pb_{3+2n}Sb_8S_{15+2n}$ which differ from other lead sulfantimonides in having tabular rather than acicular habits. Intensity data were recorded with an equi-inclination counter diffractometer. The structure was solved with the

symbolic addition procedure and refined, by least-squares techniques, to $R = 18.2\%$ for 2302 observable reflections. The asymmetric unit contains 16 atoms. Two Pb atoms are coordinated by six and seven S atoms, respectively, in octahedral-like configuration; a third Pb atom has an irregular eightfold coordination which may be described either as a square antiprism, or as a trigonal prism with neighbors along two face normals. Three of four independent Sb atoms have square pyramidal coordination; a fourth forms a trigonal pyramidal group. Of nine independent sulfur atoms, four have square pyramidal coordination, three have distorted tetrahedral coordination and two have threefold coordination. The structure is composed of slabs of PbS-like structure which are repeated by b. Stacks of such slabs exist parallel to (112) and (1$\bar{1}$2) alternately along c and extend indefinitely along [$\bar{1}$10] and [110] respectively. It is postulated that structures of other members in the homologous series contain similar slabs which differ in the width of the PbS-like unit.

Introduction

At least eighteen well-established minerals have been discovered in the system PbS—Sb_2S_3. Interestingly, with but few exceptions, they bear little similarity in either composition or crystallography to an equally complex series of lead arsenosulfides (NOWACKI, 1969; WUENSCH, 1972) even though As and Sb sulfides are often isostructural. The distinct behaviors of the lead sulfosalts undoubtedly arises from the rather different sizes of the As and Sb coordination polyhedra relative to the dimensions of the Pb—S groups. No structure had been completely determined for any lead-antimony sulfosalt when the present study was begun. A substructure for boulangerite, $Pb_5Sb_4S_{11}$, however, had been proposed by BORN and HELLNER (1960). A substructure determination for zinkenite, $Pb_6Sb_{14}S_{27}$, was subsequently reported by TAKEDA and HORIUCHI (1971).

Most of the Pb-Sb sulfosalts have been found to display one lattice constant either equal to 4 Å or, more commonly, double this value. On the basis of the structures which have been determined for boulangerite, zinkenite and a number of other antimony and bismuth sulfosalts, this lattice constant appears to correspond to the periodicity of chains of SbS_5 square pyramids sharing edges. The minerals of the plagionite group, Table 1, do not display this 4 Å periodicity. The habit of these minerals also differs from that of other lead sulfantimonides: rather than being acicular, with an axis of elongation parallel to the 4 Å translation, they are tabular to stoutly prismatic in habit. The four members of the plagionite group constitute an apparent homologous series whose compositions may be expressed $Pb_{3+2n}Sb_8S_{15+2n}$ (with $n = 0$ to 3). The probable space group for all four phases is $C2/c$.

Table 1. *The plagionite group*

		a	*b*	*c*	*β*	Reference
Fülöppite	$Pb_3Sb_8S_{15}$	13.39 Å	11.69 Å	16.91 Å	94.68°	Nuffield, 1946
Plagionite	$Pb_5Sb_8S_{17}$	13.4857	11.8656	19.9834	107.168	Present work
Heteromorphite	$Pb_7Sb_8S_{19}$	13.60	11.93	21.22	90.83	Jambor, 1969
Semseyite	$Pb_9Sb_8S_{21}$	13.603	11.936	24.453	106.05	Kohatsu, 1973

Table 1 shows that two lattice constants remain essentially invarient throughout the series, while the third increases uniformly with n. With the possible exception of fülöppite, all members of the series display a {112} cleavage of increasing ease as n increases.

The present investigation of the crystal structure of plagionite was undertaken to determine the structural relationship among members of this series. A preliminary account of the structure has been previously presented (Cho and Wuensch, 1970).

X-ray examination

Crystals of plagionite from Wolfsberg, Harz, Germany were obtained from the Harvard Collection (Catalogue No. 11391). Crystal fragments were ground into spheres of small radius in an attempt to minimize absorption effects ($\mu_l = 1197$ cm^{-1} for Cu$K\alpha$). The specimen selected for study had a radius of 0.054 ± 0.002 mm ($\mu_l r = 6.51$ for Cu$K\alpha$). Precession and Weissenberg photographs indicated that the mineral was monoclinic. Systematic absences were observed for *hkl* reflections with $h + k \neq 2n$ and *h0l* reflections with $l \neq 2n$. The diffraction symbol is thus $2/m$ *C*-/*c* which permits *Cc* and $C2/c$ as possible space groups. The centrosymmetric space group was chosen as the correct possibility on the basis of crystal morphology (Palache *et al.*, 1944). This choice was subsequently confirmed by statistical tests performed on the set of diffracted intensities (Table 3).

Precise lattice constants were determined from back-reflection Weissenberg photographs (Buerger, 1937). A least-squares extrapolation based upon 108 0*kl* and 36 *h*0*l* reflections, in which parameters characterizing systematic errors due to film shrinkage, sample eccentricity and absorption were refined, was performed with the program LCLSQ3 (Burnham, 1962). The lattice constants obtained (Table 2), are in excellent agreement with values reported by Nuffield and Peacock (1945) and Wolfe (in Palache *et al.*, 1944) as well as early morphological data (Palache *et al.*, 1944). The lattice constants

Table 2. *Lattice constants of plagionite*

	NUFFIELD and PEACOCK (1945)*	WOLFE (in PALACHE *et al.*, 1944)*	Present work
a	13.48 Å	13.4 Å	13.4857(8) Å
b	11.83	11.9	11.8656(4)
c	19.98	19.80	19.9834(7)
β	107.18°	107.22°	107.168(4)°

* Converted to Ångstroms from kx units.

Table 3. *Statistical distribution of normalized structure factors*

	Experimental	Theoretical	
		Centric	Acentric
$< \|E\| >$	0.853	0.798	0.886
$< E^2 >$	0.999	1.000	1.000
$< E^2 - 1 >$	0.874	0.968	0.736
$\|E\| > 1.0$	31.54%	32.00%	37.00%
$\|E\| > 2.0$	3.95%	5.00%	1.80%
$\|E\| > 3.0$	0.17%	0.30%	0.01%

obtained in the present work provide, for $Z = 4$, $\varrho_{\text{cal}} = 5.55$ g cm^{-3}. The measured density for material from the same locality is 5.54 g cm^{-3} (NUFFIELD and PEACOCK, 1945) while that reported for crystals from Oruro, Bolivia is 5.56(2) g cm^{-3} (BERMAN in PALACHE *et al.*, 1944).

Intensity collection

Diffracted intensities were recorded with a Buerger equi-inclination counter diffractometer equipped with a proportional counter as detector and pulse-height analysis circuitry. Data on the zero to twelveth levels were obtained through rotation of the crystal about b. Of 3579 independent reflections contained within the Cu$K\alpha$ sphere of reflection, 2953 were accessible with the diffractometer which was used. Background intensity was measured for 50 sec at φ equal to $\pm 3°$ of the diffraction maximum, and the total counts and scanning time were recorded as the crystal was rotated through 6° in φ. An intensity was considered to be below the minimum limit of detectability when the counts accumulated during a scan less the probable error ($0.6745\,\sigma$) fell below the value of the integrated background plus its probable

error. Such intensities were assigned a value equal to one-third the minimum detectable value.

The high linear absorption coefficient and small crystal volume combined to produce very weak intensities. (The strongest intensity provided a diffraction peak of only 500 counts/sec.) As a result 651 of the 2953 accessible intensities were undetectable and the data which could be recorded were subject to high standard deviations. The intensities were corrected for Lorentz, polarization, and spherical absorption factors with the aid of the programs FINTE and GAMP (ONKEN, 1964). No correction for extinction was employed.

Solution of the structure

The structure of plagionite was solved with the aid of the symbolic addition procedure. The 2302 observable structure factors were placed on an absolute scale with the aid of a Wilson plot. Normalized structure factors, E, where $|E(hkl)|^2 = |F(hkl)|^2/\varepsilon\Sigma f^2(hkl)$, and $\varepsilon = 2$ for both hkl reflections (as a result of the C lattice) and $h0l$ reflections (as a result of the c glide) were computed with the program FAME (FLEISCHER, DEWAR and STONE, 1967). The statistics of the distribution of $|E|$'s (Table 3), supports selection of the centrosymmetric space group as the correct option in accord with the morphology of the mineral. The 25 largest E's (> 2.515) were tested for Σ_2 interactions to assign optimum initial sign symbols. The symbolic addition procedure was performed with the aid of the program MAGIC (FLEISCHER *et al.*,1967) utilizing nine symbolic signs and a set of 950 E's > 0.831. After five iterations, 767 E's were assigned sign symbols. One symbol was little used and was discarded. Of 64 possible sign combinations (2^n, where n is the number of symbols less two origin-defining symbols), one indicated a contradiction index which was an order of magnitude smaller than the remaining combinations. Upon ignoring knowns containing other than the eight retained symbols, 633 E's were assigned signs at probability levels greater than 0.989.

Refinement of the structure

An E map based upon the signs obtained through the symbolic addition procedure clearly revealed the locations of four Sb atoms, all in general position $8f$, two Pb atoms in the general position and one Pb in special position $4e2$. Positions for the sulfur atoms were also suggested in the E map but their location was deferred to subsequent

difference maps computed on the basis of signs determined from the heavy-atom locations.

Refinement of the metal atom coordinates and temperature factors with the full-matrix least-squares program SFLSQ5 (PREWITT, 1962) resulted in a disagreement index, $R = \Sigma||F_{obs}| - |F_{cal}||/\Sigma|F_{obs}|$, of 27.5%. A difference map prepared at this stage revealed positions for nine sulfur atoms—eight in the general position, plus one in special position $4e2$. The sulfur atoms were incorporated in the refinement and, in addition, corrections for anomalous dispersion were made for all atoms. Further, the weighting scheme (previously based on $w = \sigma^{-2}$, where σ is the standard deviation based upon the counting statistics of the individual intensity measurements) was examined by evaluating $\Sigma w (F_{obs} - F_{cal})^2$ as a function of $|F_{obs}|$. It was found that $\Sigma w\Delta^2$ was proportional to $|F_{obs}|$; the weighting scheme adopted in subsequent cycles of refinement was adjusted such that $\Sigma w\Delta^2$ was independent of $|F_{obs}|$. Under these conditions, subsequent refinement of atomic positions, isotropic temperature factors, and a single scale factor converged to a disagreement index of 18.2%. The "weighted" R, $[\Sigma w (F_{obs}-F_{cal})^2/\Sigma w F_{obs}^2]^{1/2}$, was 20.0%. Upon inclusion of the 651 unobservable structure factors, R became 21.8%.

A difference map prepared at this stage revealed only one sort of anomaly: a classic "clover leaf" about each atom which is usually indicative of anisotropic thermal motion. However, the orientation of the anomaly was identical for every atom in the asymmetric unit. This suggested a physically unreasonable thermal motion and the anomalies were instead interpreted as arising from a systematic error in the correction for absorption. Remeasurement of the sample did indeed reveal a departure from sphericity, but the irregularity was too small (0.002 mm) to permit accurate measurement and incorporation into an improved absorption correction. In view of the large linear absorption coefficient, the variation in shape is sufficient to cause an error in the set of F_{obs} which would range from 5.84% at $\theta = 0°$ to 1.85% at $\theta = 90°$. Introduction of anisotropic thermal motion would have improved the agreement between observed and calculated structure factors. The parameters obtained, however, would have been without physical significance, and refinement was accordingly terminated at $R = 18.2\%$.

While this level of agreement would be high for a less-absorbing material, it may be satisfactorily explained in terms of the counting statistics of the data set and the uncertainty in the correction for

absorption. Figure 1 presents the average value of σ/F_{obs} (where σ is the standard deviation in a structure factor obtained from counting statistics), for groups of 75 reflections of neighboring magnitude, plotted as a function of the magnitude of F_{obs}. The value of $\Sigma\sigma/\Sigma|F_{obs}|$, a quantity analogous to R, was 8.06% for the entire data set; $\sigma/|F_{obs}|$ is greater than 10% for half of the observable data. Figure 1 also includes plots as a function of $|F_{obs}|$ of the average values of $|F_1 - F_2|/\frac{1}{2}(F_1 + F_2)$ where F_1 and F_2 are symmetry-equivalent structure

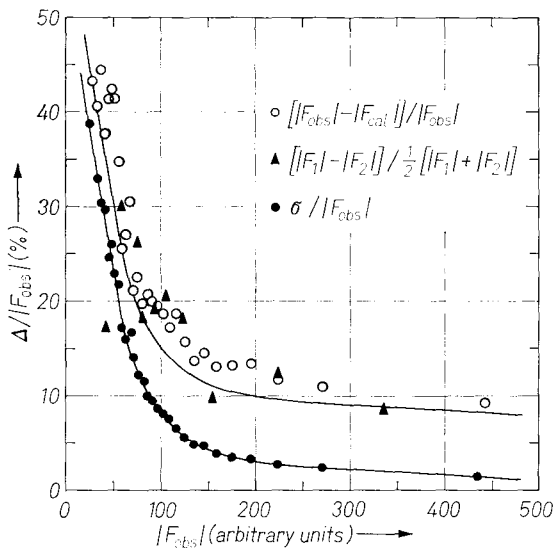

Fig. 1. Comparisons of plots, as a function of $|F_{obs}|$, of $\sigma/|F_{obs}|$ (each datum is an average of a group of 75 reflections of neighboring magnitude); $||F_{obs}| - |F_{cal}||/\Sigma|F_{obs}|$ (groups of 75 reflections) and $||F_1| - |F_2||/|\bar{F}|$, where F_1 and F_2 are measurements of equivalent structure factors (groups of eight reflections). Only the observable data are included

factors, and R, $||F_{obs}| - |F_{cal}||/|F_{obs}|$. The value of $\Sigma|F_1 - F_2|/\Sigma\frac{1}{2}(F_1 + F_2)$ was 14.9%—comparable to the value of 18.2% obtained for R. Figure 1 shows the agreement between F_{obs} and F_{cal} to be essentially that between symmetry-equivalent reflections. The upper line drawn through the plots of R and the agreement between equivalent F_{obs} is a curve obtained by the addition of 6.8%, the difference between $\Sigma|F_1 - F_2|/\Sigma\frac{1}{2}(F_1 + F_2)$ and $\Sigma\sigma/\Sigma|F_{obs}|$, to the curve describing the variation of $\sigma/|F_{obs}|$ with $|F_{obs}|$. The result is a fair

representation of the variation of R with $|F_{obs}|$. The difference between $\sigma/|F_{obs}|$ and $|F_{obs} - F_{cal}|/|F_{obs}|$ is therefore not a function of $|F_{obs}|$, and turns out to be comparable (although slightly larger) to the 5.8% to 1.9% error introduced by the uncertainty in the correction for absorption.

Results of the refinement

The asymmetric unit of plagionite contains sixteen atoms: 2Pb, 4Sb and 8S atoms located in general position $8f$, plus 1Pb and 1S atom in special position $4e2$. The atomic positions and isotropic temperature factors are presented in Table 4. The parameters reported are those of CHO and WUENSCH (1970), but the asymmetric unit has been redefined in order to emphasize features of the structure which are discussed in the following section. The relation between the present designation of the asymmetric unit and that previously reported is

Pb(1) = Pb(3^4)	Sb(3) = Sb(2^3)	S(4) = S(8^2)
Pb(2) = Pb(2^2)	Sb(4) = Sb(3^3)	S(5) = S(1^3)
Pb(3) = Pb(1^6)	S(1) = S(9^2)	S(6) = S(6^1)
Sb(1) = Sb(1^4)	S(2) = S(2^4)	S(7) = S(7^1)
Sb(2) = Sb(4^3)	S(3) = S(3^4)	S(8) = S(4^3)
		S(9) = S(5^3)

Table 4. *Atomic positions and temperature factors for plagionite* (estimated standard deviations in parentheses)

Atom	x	y	z	B
Pb(1)	−0.5	0.6801(4)	0.75	2.68(7) Å^2
Pb(2)	−0.2310(2)	0.6259(2)	0.6780(2)	2.18(4)
Pb(3)	0.2634(3)	0.4138(3)	0.5516(2)	2.67(5)
Sb(1)	0.0018(4)	0.5184(4)	0.6053(3)	2.54(8)
Sb(2)	0.4906(3)	0.3047(3)	0.4715(2)	1.77(6)
Sb(3)	0.7290(4)	0.1904(4)	0.4143(2)	1.83(6)
Sb(4)	0.9539(3)	0.1250(4)	0.3329(2)	1.80(6)
S(1)	−1.0	0.7431(23)	0.75	2.4(4)
S(2)	−0.8188(14)	0.7338(14)	0.6709(9)	2.1(3)
S(3)	−0.6113(10)	0.6387(11)	0.6017(7)	1.5(2)
S(4)	−0.3699(14)	0.5258(14)	0.5583(9)	1.9(2)
S(5)	−0.1087(12)	0.4160(13)	0.4991(9)	1.7(2)
S(6)	0.1314(12)	0.3104(12)	0.4367(8)	1.6(2)
S(7)	0.3812(12)	0.1926(13)	0.3759(8)	2.2(3)
S(8)	0.6135(11)	0.0766(11)	0.3210(8)	1.7(2)
S(9)	0.8532(14)	−0.0046(14)	0.2438(10)	2.0(2)

Table 5. *Comparison of observed and calculated structure factors* (asterisk indicates unobservable structure factors which were assigned values estimated from one-third the minimum observable intensity)

l	$\lvert F_o\rvert$	$\lvert F_c\rvert$	l	$\lvert F_o\rvert$	$\lvert F_c\rvert$	l	$\lvert F_o\rvert$	$\lvert F_c\rvert$	l	$\lvert F_o\rvert$	$\lvert F_c\rvert$	l	$\lvert F_o\rvert$	$\lvert F_c\rvert$	l	$\lvert F_o\rvert$	$\lvert F_c\rvert$	l	$\lvert F_o\rvert$	$\lvert F_c\rvert$	l	$\lvert F_o\rvert$	$\lvert F_c\rvert$
0 0 1			-4	132	198	2	472	458	6	414	376	15	170	166	11	207	293	13	338	347	-19	160	182
-2	1229	1214	3*	84	20	7	165	160	11 1 1						12	240	264	14	211	94	-18	195	186
2 297	266	0	1551	1351	4	1205	1148	8*	55	11					13	417	504	15	125	68	-17	86	59
4 236	108	2	362	397	5	1044	959	9*	52	104	-22	103	115		14	139	7	16	151	151	-16*	39	15
6* 85	102	4	192	181	6	311	237	10	128	128	-21	111	173		15	181	171	17	300	268	-15	77	149
8 506	623	6	663	735	7	258	243	11*	55	62	-20	252	271		16	180	165	18	332	348	-14	188	254
10 294	360	8	241	234	8*	62	112	12	365	373	-19	262	269		17	232	284	19	70	75	-13*	46	103
12 541	642	10	252	315	9*	59	4	13	152	179	-18	322	347		18	325	443	20*	28	54	-12*	50	12
14 1076	995	12	167	227	10*	57	70	14	293	233	-17	126	119		19	91	0	6 2 1			-11	162	154
16 183	189	14	396	443	11*	56	3	15	198	206	-16*	47	29		20	196	281				-10	214	178
18 143	226	16	299	344	12	170	230	16	170	125	-15	252	318		21*	32	24	-24	75	64	-9*	51	165
20 79	30	10 0 1			13	209	204	17	308	295	-14	95	106		22	100	86	-23*	30	41	-8	144	261
22 82	78				14	312	312	18	137	198	-13	186	181		23	74	20	-22*	32	24	-7	247	251
		-22	116	168	15*	58	113	19	216	187	-12*	44	27					-21	108	8	-6	193	99
2 0 1		-20	174	237	16*	50	92	20	77	58	-11*	47	31		2 2 1			-20*	40	89	-5	493	484
-24 59	108	-18	208	382	17	526	540	7 1 1			-10*	49	148	-23	72	39	-19	163	275	-4	370	366
-22* 40	666	-16	121	153	18	269	322				-9	162	194	-22	139	175	-18*	42	108	-3	239	309
-20 121	213	-14	167	197	19	233	190	-24	62	51	-8	120	122	-21*	38	100	-17	224	259	-2	174	147
-18 163	184	-12	154	128	20	118	14	-23*	33	23	-7	420	433	-20*	35	38	-16	91	36	-1*	51	89
-16 108	299	-10	817	943	21*	37	23	-22	121	84	-6	345	367	-19	246	437	-15	196	227	0*	52	157
-14 207	275	-8	743	736	22*	30	82	-21	105	134	-5*	51	101	-18*	41	87	-14	142	252	1	415	412
-12* 55	46	-6	474	506		3 1 1		-20*	44	45	-4	243	246	-17	103	101	-13	115	25	2*	52	49
-10 171	211	-4	135	174				-19	122	182	-3	198	200	-16*	53	78	-12	122	220	3	679	602
-8 1573	1589	-2	344	406	-24	108	174	-18	402	506	-2	152	165	-15*	55	70	-11	308	342	4	413	360
-6 233	221	0	107	36	-23	62	15	-17	282	424	-1	239	282	-14	121	97	-10	436	522	5*	56	44
-4* 167	120	2	461	504	-22*	37	124	-16	112	23	0	190	158	-13	235	385	-9*	54	41	6*	41	84
-2 254	345	4	132	118	-21	85	47	-15	251	414	1	307	281	-12	106	166	-8*	56	155	7	118	103
0* 95	149	6*	46	22	-20*	42	84	-14*	56	145	2	212	198	-11	213	223	-7	238	274	8	111	149
2 285	185	8	358	412	-19*	43	126	-13*	54	190	3*	43	39	-10	560	628	-6	565	603	9	284	223
4* 183	465	10	224	188	-18	223	315	-12*	54	72	4	100	38	-9	314	370	-5	1442	1460	10	512	463
6 176	102	12*	33	29	-17	452	594	-11*	54	60	5	122	44	-8	147	164	-4	788	784	11	290	248
8 935	912	14*	27	108	-16*	52	156	-10*	53	78	6*	43	72	-7	512	524	-3*	74	221	12	60	50
10 150	67	12 0 1			-15	257	343	-9*	54	105	7	437	412	-6	150	111	-2	146	32	13	188	152
12* 55	65				-14	110	276	-8	150	192	8	77	112	-5	1468	1380	-1*	63	54	12 2 1			
14 201	276	-20*	28	16	-13*	57	58	-7	520	593	9	258	224	-4	677	630	0	150	164			
16 194	282	-18*	32	78	-12*	60	128	-6	220	234	10	102	86	-3*	26	25	1	264	291	-21	97	89
18 114	117	-16	124	162	-11*	56	104	-5	306	343	11	128	134	-2	155	65	2*	61	75	-20	150	154
20 96	74	-14	216	282	-10	158	96	-4	644	658	12	148	160	-1*	75	158	3	1057	967	-19	210	251
22 292	354	-12*	44	23	-9*	61	107	-3	616	640				0*	78	108	4	523	414	-18	158	159
4 0 1		-10	193	251	-8*	68	207	-2	248	221	13 1 1			1	244	214	5	161	132	-17	188	170
		-8	254	340	-7	498	554	-1	422	509	-20*	27	43	2*	75	11	6*	56	31	-16	97	140
-24 106	156	-6*	47	68	-6	977	1056	0	145	18	-19	60	84	3	1337	1112	7	456	394	-15	129	121
-22* 36	60	-4	377	420	-5	1046	1170	1*	61	262	-18	81	57	4	1489	1176	8	317	307	-14	136	124
-20 98	38	-2	529	528	-4	630	755	2	350	354	-17	79	166	5	1756	1431	9	718	574	-13	352	436
-18 112	51	0	188	211	-3	442	572	3	210	178	-16	264	274	6	170	192	10	466	430	-12	196	239
-16 251	387	2	288	310	-2*	84	189	4*	55	8	-15	453	436	7	720	611	11	469	412	-11	262	348
-14 509	650	4*	60	59	-1	201	376	5	169	172	-14	242	224	8	148	96	12*	49	17	-10	211	258
-12 242	306	6	402	463	0	147	57	6*	53	2	-13	204	253	9	623	533	13	128	130	-9	250	259
-10 462	599	8*	32	51	1	160	6	7	409	366	-12	187	136	10	814	763	14*	38	39	-8	102	17
-8* 65	165	10	84	88	2	279	333	8	198	180	-11	123	44	11*	58	67	15	159	129	-7	180	212
-6* 75	106				3	324	201	9	863	744	-10	187	199	12	302	312	16	173	138	-6	149	122
-4* 81	39	14 0 1			4	201	222	10	177	199	-9	163	173	13	256	282	17	234	255	-5	675	632
-2* 187	780	-18	271	356	5	173	98	11	83	65	-8	75	50	14	181	136	18*	32	37	-4	280	321
0 1797	1655	-16	197	234	6	179	175	12	326	333	-7	119	162	15	228	212		8 2 1		-3	103	132
2 511	468	-14	158	135	7	113	191	13	282	261	-6	126	166	16	214	233				-2*	43	49
4* 67	113	-12	61	62	8	597	502	14*	41	14	-5*	43	91	17*	40	42	-23*	30	63	-1	242	270
6 347	381	-10	410	408	9	964	840	15	224	109	-4	240	298	18	103	179	-22	91	204	0*	44	12
8 584	584	-8	123	136	10	223	200	16	155	142	-3*	43	43	19	426	395	-21	100	67	1	218	210
10 150	84	-6	386	443	11	135	66	17	273	275	-2	109	12	20	115	66	-20	222	312	2	192	186
12 160	138	-4	177	222	12	642	607	18	53	75	-1	89	81	21	287	286	-19	230	331	3	389	375
14 758	761	-2	385	394	13	351	313		9 1 1		0	97	103	22	84	44	-18	315	422	4	156	198
16* 42	22	0	74	108	14	161	226				1	129	112		4 2 1		-17*	41	6	5	263	219
18 207	148	2	356	332	15*	47	20	-23	168	240	2	244	257				-16*	47	74	6	63	72
20 73	20	4	113	32	16	149	155	-22	150	224	3	116	68	-24	96	130	-15*	53	15	7	282	246
6 0 1		6	112	152	17	225	240	-21*	35	50	4	357	364	-23	89	69	-14	309	316	8	70	12
		16 0 1			18*	40	8	-20	150	212	5	240	197	-22	104	92	-13	678	818	9*	32	17
-24 171	297				19	194	174	-19	127	119	6	82	38	-21	131	267	-12	165	209	10	74	53
-22 372	534	-12*	26	84	20	358	374	-18*	43	29	7	99	58	-20	124	207	-11	94	205		14 2 1	
-20 151	278	-10	133	160	21*	28	34	-17*	44	96	8	136	92	-19	129	257	-10	215	140			
-18 219	386	-8	87	116		5 1 1		-16*	45	51	15 1 1			-18	337	491	-9*	57	18	-18	124	150
-16 206	251	-6	113	110	-15	214	265	-15	214	265				-17	186	286	-8*	56	81	-17	125	135
-14* 51	33	-4	236	254	-24	84	86	-14	308	401	-16	142	138	-16*	51	103	-7*	51	45	-16*	31	45
-12 103	25	-2	263	283	-23	97	195	-13	473	570	-15*	28	44	-15	311	337	-6*	57	62	-15	111	106
-10* 56	109		1 1 1		-22	190	266	-12	241	267	-14	76	74	-14*	50	35	-5	386	405	-14*	33	79
-8 987	1209				-21*	40	103	-11	147	143	-13	139	136	-13	622	772	-4	312	328	-13	82	32
-6 452	539	-23*	28	43	-20	92	84	-10	570	655	-12	245	229	-12	437	481	-3	103	60	-12*	36	52
-4* 61	34	-22	231	309	-19	173	252	-9	325	390	-11*	42	119	-11	128	174	-2*	65	5	-11	111	94
-2 268	365	-21	70	55	-18	110	94	-8*	58	112	-10	78	120	-10	211	187	-1	554	571	-10*	40	32
0 122	146	-20	115	129	-17	93	4	-7	117	197	-9	288	291	-9*	60	24	0*	52	44	-9	144	180
2* 61	52	-19	148	266	-16	124	115	-6	297	360	-8	81	45	-8*	63	38	1	203	168	-8	116	157
4 629	613	-18*	49	142	-15	262	350	-5*	54	19	-7	168	162	-7*	62	44	2*	55	105	-7	232	254
6 183	180	-17	120	168	-14	542	681	-4	153	155	-6	196	174	-6*	65	18	3	417	408	-6	222	236
8 629	601	-16*	51	18	-13	433	520	-3	66	37	-5	204	181	-5	565	705	4	209	200	-5	271	261
10 212	125	-15*	54	88	-12	193	290	-2	321	380	-4	231	230	-4	827	819	5*	50	11	-4	285	318
12 133	103	-14*	58	264	-11	105	157	-1*	60	21	-3*	35	60	-3	844	866	6*	53	18	-3	221	210
14 331	405	-13	400	521	-10	697	751	0	322	363	-2	153	152	-2	203	163	7	237	197	-2*	37	34
16* 36	67	-12	381	502	-9	447	546	1	446	449	-1	69	43	-1	567	570	8	312	209	-1*	40	57
18 189	165	-11	534	624	-8*	60	47	2	178	166	0*	30	14	0	224	222	9	186	157	0	73	42
8 0 1		-10	945	1051	-7*	64	261	3	286	220	1	225	218	1*	67	126	10*	41	86	1	409	393
		-9	774	883	-6	182	222	4	615	569	2	138	110	2	210	190	11*	48	51	2	75	73
-24* 24	111	-8	122	150	-4*	72	185	5	305	257	3	150	152	3	637	645	12*	36	36	3	172	155
-22 103	129	-7	195	230	-3*	69	75	6	249	232	2*	67	127	4	587	466	13	225	183	4*	31	83
-20* 40	111	-6*	88	24	-2	281	338	7	218	197	3	648	626	5	107	221	14	246	154	5	108	94
-18* 44	35	-5	204	189	-1*	71	177	8*	44	20	4	274	221	6*	62	30	15	131	89			
-16* 49	65	-4	168	319	0*	71	98	9	82	16	5*	81	72	7	231	164	16	121	126		16 2 1	
-14 234	337	-3*	84	49	1*	67	37	10*	44	144	6*	65	49	8*	58	193		10 2 1		-11	170	190
-12 196	235	-2*	78	36	2	198	82	11	111	83	7	128	115	9	390	332				-10	116	93
-10 438	650	-1	141	80	3	124	99	12	452	387	8*	63	104	10	123	156	-22*	33	84	-9	137	132
-8 211	288	0	192	94	4	1403	1229	13	156	112	9	173	118	11	248	251	-21*	32	6	-7	268	266
-6 187	162	1	237	205	5	1106	936	14*	32	26	10*	60	85	12	346	278	-20	73	25	-6	92	57

Table 5. *(Continued)*

l	$\|F_o\|$	$\|F_c\|$	l	$\|F_o\|$	$\|F_c\|$	l	$\|F_o\|$	$\|F_c\|$	l	$\|F_o\|$	$\|F_c\|$	l	$\|F_o\|$	$\|F_c\|$	l	$\|F_o\|$	$\|F_c\|$	l	$\|F_o\|$	$\|F_c\|$
-5	70	49	-20	86	69	-6	172	217	-2	100	51	1	257	148	13	108	124	-17	140	128	-7	160	228
-4	187	189	-19*	45	1	-5	144	238	-1	164	121	2	733	712	14	113	45	-16	115	217	-6	414	432
-3	304	290	-18*	46	26	-4	215	256	0	315	267	3*	53	19	15	221	153	-15*	59	3	-5	215	246
1	3	1	-17	116	131	-3	417	392	1	176	149	4	685	648	10	4	1	-14	102	215	-4*	50	1119
			-16	94	118	-2	353	358				5	844	673				-13*	53	165	-3	188	160
-23*	26	46	-15*	52	57	-1	376	372	0	4	1	6	258	221	-21*	36	26	-12*	55	371	-2	190	188
-22*	32	304	-14*	50	11	0*	53	15	2	222	257	7	460	375	-20	134	128	-11	161	128	-1	345	313
-21*	37	101	-12	107	82	1*	53	47	3	247	207	8	1112	912	-19	130	118	-10	162	204	0	106	21
-20*	40	113	-11*	53	49	2	106	130	4*	59	60	9	748	582	-18	302	341	-9	167	230	1*	51	8
-19*	42	59	-10	564	661	3	172	153	5	730	710	10*	55	83	-17	504	575	-8	96	29	2	192	255
-18	117	116	-9	286	340	4	409	334	6	832	804	11	260	215	-16	257	292	-7	690	721	3*	58	10
-17*	47	104	-8	605	662	6	422	360	7	704	720	12	147	80	-15	235	263	-6	295	348	4	344	295
-16	225	287	-7*	62	90	7	309	296	8	702	730	13	251	232	-14	412	401	-5	106	115	5	446	365
-15	145	60	-6	118	216	8	421	337	9	647	635	14	277	188	-12	146	202	-4	2034	1960	6	157	78
-14	111	258	-5	147	200	9	149	114	10	170	216	15	318	261	-11	172	228	-2	102	206	7	211	155
-13	103	42	-4	147	70	10*	40	73	11	154	156	16	496	455	-10	164	203	-1	109	196	8	316	265
-12	145	332	-3	451	505	11*	40	107	12	254	265	17	77	66	-9*	53	24	0*	34	34	9	226	226
-11	123	11	-2	839	812	12	328	270	13*	54	20	18	75	17	-8*	61	130	1*	36	35	10	585	447
-10	397	467	-1	866	865	13*	35	72	14	203	215	19*	30	6	-7*	61	31	2*	50	115	11*	48	33
-9	394	483	0	474	440	14	282	277	15	339	389	6	4	1	-6	398	426	3	338	371	12*	61	56
-7	223	281	1*	58	64	15	148	150	16	110	145				-5	132	192	4	236	277	13	95	78
-6	157	184	2	543	464	11	3	1	17*	48	6	-23	207	312	-4	284	255	5	694	695	14	195	88
-5	195	37	3	239	201				18	234	253	-22	85	125	-3	218	240	6	252	202	15*	40	23
-4*	67	135	4	551	462	-21*	27	68	19	117	14	-21	73	83	-2	320	260	7	312	281	16	103	70
-3	151	123	5	233	244	-20	62	8	20	130	154	-20	82	149	-1	176	174	8	360	375	17*	35	30
-2	381	475	6	350	288	-19	145	157	21	138	118	-19	81	8	0	483	406	9	104	61	18	87	73
-1*	52	906	7	664	574	-18	260	267	22	157	208	-18	313	382	1	142	55	10	320	279			
0	880	832	8	353	270	-17*	37	11				-17	368	372	2	316	258	11	484	478	7	5	1
1	347	396	9	173	142	-16	114	148	2	4	1	-16*	59	61	3	180	153	12	308	316	-22	96	149
2	518	496	10	153	140	-15	222	240	-23	166	255	-15	221	282	4	194	170	13	123	40	-21	84	119
3	247	232	11*	54	52	-14	279	288	-22	155	212	-14	559	635	5*	47	34	14*	54	48	-20	95	61
4	173	242	12	472	409	-13	79	11	-21	122	164	-13	268	328	6*	44	18	15*	53	115	-19	100	76
6	180	190	13	333	298	-12	189	177	-20	96	17	-12	124	213	7*	45	10	16	133	61	-18*	42	93
7	570	587	14	414	378	-11	329	300	-19*	54	124	-11	207	261	8	363	248	17	266	202	-17	157	153
8	375	360	15	253	224	-10	215	206	-18	94	97	-10*	56	27	9	360	266	18	99	74	-16*	51	16
9	851	787	16	176	122	-9	266	308	-17	444	567	-9*	54	110	10	114	74	19	352	340	-15	190	238
10	450	485	17	190	198	-8*	52	141	-16	110	120	-8	167	256	11	207	153	20	86	35	-14*	52	31
11	122	106	18	178	83	-7	259	253	-15	392	500	-7	184	147	12*	30	37	21	75	31	-13	424	440
12*	56	22	19*	27	5	-6	236	250	-14	435	499	-6	258	343	13	348	273				-12	319	383
13	377	368	7	3	1	-5*	49	38	-13	441	512	-5	245	283				3	5	1	-11	246	254
14	804	739				-4	100	123	-12*	55	96	-4	136	188	12	4	1				-10	213	228
15	148	96	-23	155	205	-3	143	150	-11*	60	51	-3	135	160	-19	146	178	-22	51	64	-9	95	99
16	224	213	-22*	31	55	-2*	51	16	-10*	56	91	-2*	53	32	-18*	30	14	-21*	37	46	-8*	50	57
17	236	286	-21*	40	60	-1	701	622	-9*	55	97	-1	104	160	-17	64	6	-20	86	58	-7	152	174
18	183	162	-20*	40	101	0	749	645	-8	255	326	0	1053	916	-16	81	60	-19	76	136	-6	297	360
19	96	11	-19	78	153	1*	43	20	-7	212	274	1	496	465	-15	78	62	-18*	44	159	-5*	60	118
20	180	192	-18	263	341	2	184	149	-6*	55	3	2*	60	13	-14*	38	2	-17	248	277	-4	138	78
21	113	130	-17*	44	43	3	90	27	-5	226	271	3	217	211	-13	204	232	-16*	57	22	-3	496	506
22*	27	42	-16	218	270	4*	43	53	-4*	57	25	4	203	129	-12	129	150	-15	348	412	-2*	52	8
3	3	1	-15	328	384	5	243	179	-3	156	223	5	118	78	-11	318	298	-14	165	58	-1*	55	287
			-14	447	472	6	411	352	-2	334	382	6*	55	54	-10	306	302	-13*	69	85	0	372	396
-23	261	334	-13	134	142	7	353	292	-1	461	506	7	203	156	-9	575	526	-12*	53	80	1	390	364
-22	104	136	-12	154	100	8	163	65	0	708	680	8	302	227	-8*	46	40	-11	307	361	2	522	434
-21*	37	41	-11	438	500	9	84	62	1*	54	60	9	315	241	-7	152	92	-10	203	256	3	190	134
-20*	46	157	-10	519	556	10*	33	5	2	123	34	10*	45	8	-6	121	80	-9	128	101	4	922	747
-19	90	7	-9	693	804	11	227	203	3	261	240	11	101	180	-5	116	98	-8	148	115	5	554	437
-18	115	174	-8	297	297				4	239	197	12*	51	44	-4	103	160	-7	115	54	6	185	101
-17	319	470	-7	162	134	13	3	1	5	257	209	13*	50	388	-3	171	187	-6	236	296	7	236	183
-16*	52	28	-6	260	221	-19	59	62	6	104	132	14	239	225	-2	140	165	-5	455	502	8	221	149
-15	202	220	-5	114	83	-18*	29	37	7	314	254	15	164	196	-1*	49	47	-4*	47	88	9	221	149
-14	488	564	-4*	60	23	-17*	32	67	8	204	228	16	66	83	0	158	190	-3	554	634	10	557	458
-13	266	371	-3*	55	94	-16*	36	84	9	228	207	17	157	161	1	168	156	-2*	46	9	11	276	169
-12	129	47	-2*	56	60	-15	202	234	10	202	185	18*	27	71	2*	40	15	-1	176	170	12	130	147
-11	124	149	-1	704	682	-14*	37	71	11*	55	52	8	4	1	3	207	140	0	157	157	13	295	234
-10*	60	141	0	762	682	-13	105	100	12	324	276				4	280	203	1	206	204	14	103	18
-9	738	709	1*	55	94	-12	234	229	13	607	538	-22	131	157	5	442	329	2	737	666	15	61	73
-7	243	289	2*	55	21	-11*	42	53	14	216	206	-21	84	66	6	279	219	3	482	425	16	135	155
-6	126	197	3	170	145	-10*	42	65	15	171	180	-20*	38	34	7	92	72	4	1130	698			
-5	231	360	4*	53	71	-9	311	296	16	220	204	-19	151	174	8	137	147	5*	51	29			
-4*	64	53	5*	53	59	-8	357	385	17	87	80	-18	121	142	9	89	38	6	125	123	9	5	1
-3	252	332	6	166	81	-7	165	179	18*	40	56	-17*	44	111				7	385	347	-21	149	201
-2	386	465	7	562	467	-6	113	118	19	288	259	-16	139	158	14	4	1	8*	54	14	-20	253	263
-1	757	806	8	218	52	-5	137	183	20*	34	56	-15	146	208	-16	261	257	9	358	251	-19	74	25
0	1596	1426	9	216	101	-4	255	250	21	132	187	-14*	50	32	-15	66	71	10	320	303	-18	133	176
1	1752	1195	10	97	12	-3	229	129				-13	168	252	-14	102	100	11	292	238	-17	136	111
2	384	395	11	251	172	-2	141	97	4	4	1	-12	92	100	-13	61	17	12	350	364	-16	103	130
3	190	184	12	248	154	-1	299	257	-23	71	16	-11	123	114	-12	183	155	13	161	123	-15*	46	28
4*	64	92	13*	40	57	0	165	71	-22*	32	10	-10	488	425	-11	119	144	14*	58	24	-14	299	384
5	150	197	14	325	310	1	398	180	-21	76	127	-9	536	530	-10	175	185	15*	42	40	-13	90	130
6	340	248	15	119	31	2	204	155	-20*	42	55	-8*	58	35	-9	113	121	17*	45	16	-11	187	102
7	115	81	16	88	56	3	317	272	-19*	46	129	-7	202	228	-8	255	265	18	476	426	-10*	62	96
8	138	124	17	121	85	4	131	66	-18	190	231	-6	382	372	-7*	43	8	19	68	14	-9*	51	64
9	483	458	9	3	1	5	178	136	-17	112	8	-5	222	230	-6*	39	75	20	86	86	-8	128	38
10	450	379				6	177	158	-16*	47	31	-4	125	186	-5	138	166				-7	336	383
11	264	219	-22	276	338	7	248	182	-15	326	371	-3	277	242	-4	292	232	5	5	1	-6	1023	958
12	512	451	-21	63	91				-14*	67	44	-2	350	375	-3	142	124	-22	88	95	-5*	58	188
13	160	124	-20	146	222	15	3	1	-13*	55	8	-1*	52	21	-2	338	279	-21*	35	86	-4	432	858
14	404	397	-19*	41	35	-15	126	132	-12	216	228	0*	66	16	-1	149	132	-20	355	405	-3	268	242
15	200	117	-18	124	44	-14	239	217	-11	214	240	1	287	273	0	293	241	-19*	40	44	-2	140	242
16*	46	22	-17	101	126	-13	113	123	-10	934	962	2	439	409	1	177	133	-18	382	466	-1	221	206
17	212	222	-16	128	150	-12	260	265	-9	956	971	3*	54	60	2	222	162	-17*	45	10	0	144	90
18	115	14	-15*	45	72	-11	372	355	-8	271	286	4	495	395	3	112	97	-16	104	157	1*	56	27
19*	39	112	-14	115	43	-10	267	235	-7	437	421	5	815	655	4	170	104	-15	148	111	2	407	387
20	233	197	-13	118	56	-9	76	101	-6	538	597	6*	52	15	1	5	1	-14	250	314	3	199	116
21	87	93	-12*	57	115	-8*	35	30	-5	448	520	7	496	404				-13	239	176	4	241	119
5	3	1	-11*	51	30	-7	164	160	-4*	60	241	8	480	396	-22	67	105	-12	203	239	5	285	228
			-10	167	186	-6*	32	34	-3	334	320	9	258	198	-21	125	180	-11	172	217	6	403	339
-23	105	205	-9	145	170	-5*	48	40	-2*	56	135	10	305	222	-20*	37	51	-10*	50	15	7	264	232
-22	396	512	-8	651	662	-4	118	110	-1	144	145	11	293	238	-19*	43	13	-9*	54	21	8*	44	65
-21	123	189	-7	121	39	-3	275	249	0	420	442	12	121	80	-18	548	638	-8*	50	14	9	260	198

Table 5. *(Continued)*

l	$\lvert F_o\rvert$	$\lvert F_c\rvert$
10	252	163
11	100	50
12	316	246
13*	32	12
	11 5 1	
-20*	27	4
-19	137	138
-18	152	113
-17	65	51
-16	68	53
-15	233	257
-14	281	257
-13	403	369
-12	136	135
-11	97	82
-10	246	237
-9*	51	21
-8*	60	20
-7*	48	133
-6*	48	131
-5	229	228
-4*	58	135
-3	184	185
-2	243	240
-1	366	308
0	398	318
1	477	398
2	413	317
3*	49	32
4	247	196
5	190	120
6	245	164
7	176	120
8	90	93
9*	43	36
10	251	220
	13 5 1	
-17*	29	75
-16*	30	4
-15	84	64
-14	194	192
-13*	31	50
-12	126	166
-11	151	160
-10	76	49
-9	161	159
-8	284	253
-7	123	153
-6	510	418
-5	101	116
-4	220	152
-3	173	153
-2	289	256
-1	87	17
0*	59	43
1	137	92
2	405	318
3*	34	14
4*	33	93
5	254	184
6	210	163
	15 5 1	
-11*	28	12
-10	250	219
-9	72	64
-8	68	84
-7	59	22
-6	172	171
-5	153	133
-4	76	101
-3	80	83
-2	331	230
	0 6 1	
2	177	219
3*	37	67
4	164	160
5	344	366
6	512	506
7	99	84
8	490	481
9	568	573
10	222	256
11	142	30
12	220	242
13*	51	22
14	179	184
15	110	15
16	140	159
17	177	174
18	279	310
19*	38	29
20*	35	36
21	198	275
	2 6 1	
-21	133	174
-20	125	194
-19	87	42
-18	98	192
-17*	44	67
-16*	45	52
-15	161	127
-14	301	471
-13	556	695
-12	220	271
-11	227	305
-10	300	331
-9*	56	76
-8	109	93
-7	233	344
-6*	49	102
-5	158	242
-4	148	200
-3	414	458
-2	204	268
-1	508	622
0	680	665
1	1188	1040
2	271	227
3	104	24
4	232	195
5	137	3
6	233	204
7	367	330
8	163	130
9	325	304
10	395	358
11*	53	161
12	251	254
13	735	659
14	209	173
15	308	279
16	130	99
17	81	12
18	80	142
19	64	74
20	120	153
	4 6 1	
-22	84	121
-21	195	291
-20	100	170
-19	134	239
-18	117	189
-17	105	141
-16*	56	143
-15*	48	126
-14*	53	22
-13*	50	40
-12	413	487
-11	420	481
-10	322	410
-9	558	610
-8	354	336
-7	423	499
-6*	52	34
-5	154	123
-4	189	166
-3	88	56
-2	163	122
-1	114	54
0	212	149
1*	48	21
2	314	254
3	146	104
4	192	44
5	259	234
6	122	113
7	96	92
8	438	384
9	532	424
11	207	182
12	282	238
13*	41	91
14	322	265
15*	46	69
16	144	160
17	111	128
18	250	224
	6 6 1	
-22*	27	70
-21	84	46
-20	219	287
-19	118	146
-18*	40	50
-17	113	60
-16	104	62
-15*	49	119
-14	345	328
-13	373	429
-12	236	266
-11	224	229
-10	104	156
-9	251	261
-8	154	168
-7*	49	6
-6*	59	36
-5	124	127
-4	454	471
-3	703	621
-2	184	171
-1	150	148
0	641	578
1	1026	830
2	242	220
3	182	192
4	137	87
5	316	261
6	354	298
7	203	145
8*	48	32
9	365	306
10	443	329
11	341	311
12*	42	44
13	504	404
14	91	106
15	275	246
16	189	166
	8 6 1	
-21	261	338
-20	64	116
-19	265	301
-18	147	199
-17	87	106
-16	101	75
-15*	42	44
-14*	47	14
-13	167	153
-12	331	346
-11	495	493
-10	172	133
-9	266	324
-8*	51	128
-7	384	386
-6	381	387
-5	454	443
-4	133	108
-3	146	75
-2	183	142
-1	174	115
0	265	238
1	233	224
2	184	116
3	277	242
4	204	96
5	658	481
6	111	62
7	98	13
8	441	325
9	312	244
10*	47	46
11	129	75
12	84	6
13	144	110
14	294	257
	10 6 1	
-20	143	181
-19	53	40
-18	62	40
-17*	37	112
-16	489	257
-15	236	206
-14	418	395
-13	172	189
-12	208	227
-11*	45	127
-10*	52	45
-9	167	233
-8	267	272
-7*	49	10
-6	103	5
-5*	49	67
-4	135	49
-3	272	211
-2	261	215
-1	280	230
0	311	239
1	404	308
2	114	44
3	154	132
4*	47	39
5	334	252
6	394	286
7	103	103
8	216	167
9	116	61
10	202	122
11	396	354
	12 6 1	
-17	120	176
-16	75	78
-15*	36	40
-14*	37	40
-13	139	147
-12	176	242
-11	571	531
-10	150	127
-9	84	20
-8	74	87
-7	310	257
-6	136	100
-5	198	212
-4*	43	24
-3	219	218
-2	98	83
-1*	40	62
0	102	56
1	115	68
2	138	101
3	407	298
4	160	79
5	167	93
6	95	66
7	99	106
	14 6 1	
-13	134	186
-12*	32	32
-11*	32	2
-10	77	20
-9*	33	100
-8	164	161
-7	63	68
-6	102	83
-5	131	124
-4	224	192
-3	123	95
-2	73	57
-1	198	128
0	372	287
1	203	165
	1 7 1	
-20	72	79
-19	94	117
-18	195	222
-17	104	105
-16	114	164
-15	154	152
-14	89	136
-13	127	203
-12	266	234
-11	115	73
-10	269	278
-9	131	154
-8	298	309
-7*	44	19
-6	430	473
-5	159	180
-4	168	223
-3	230	290
-2*	28	44
-1	562	670
0*	24	65
1*	30	59
2	554	540
3	179	140
4	107	67
5	246	228
6	163	181
7	494	512
8	537	496
9	496	538
10*	53	92
11	401	377
12	275	281
13	314	278
14	283	308
15	76	27
16	362	395
17*	37	106
18	79	51
19*	28	66
	3 7 1	
-21*	26	23
-20	64	10
-19*	40	52
-18	80	35
-17*	44	42
-16	260	358
-15	110	136
-14	278	354
-13*	49	132
-12*	47	34
-11	315	328
-10*	50	63
-9	724	819
-8	415	461
-7	291	302
-6	119	130
-5	181	204
-4*	40	52
-3	178	168
-2	456	464
-1	624	626
0	334	322
1	720	682
2*	42	23
3	599	512
4	80	10
5	357	291
6	603	554
7	139	76
8*	53	50
9*	47	5
10	227	228
11*	50	63
12	110	106
13	149	122
14	84	95
15*	44	56
16	139	164
17	193	259
18	158	152
	5 7 1	
-21*	28	20
-20*	32	58
-19	127	118
-18	100	22
-17	232	292
-16	348	427
-15*	42	47
-14	172	202
-13	147	242
-12*	47	50
-11	189	188
-10	329	354
-9	109	58
-8	338	333
-7	101	53
-6	170	183
-5	169	194
-4	173	215
-3	113	89
-2	145	141
-1	766	715
0	673	596
1*	45	22
2	527	505
3	158	105
4	205	178
5	494	408
6	438	330
7	582	513
8	276	226
9	282	254
10	227	171
11	230	238
12*	43	94
13	327	274
14	280	292
15	166	127
16	212	227
	7 7 1	
-20	66	83
-19	79	84
-18	73	73
-17	85	174
-16	292	381
-15	195	253
-14	224	261
-13*	52	30
-12*	45	55
-11*	48	91
-10	351	345
-9	839	866
-8	357	375
-7*	46	42
-6	164	175
-5*	50	125
-4	167	69
-3	273	206
-2	211	169
-1	461	444
0*	48	35
1	182	122
2	195	149
3	591	489
4	288	241
5	450	356
6	293	258
7	192	153
8	105	62
9	170	115
10*	41	49
11	186	150
12	108	44
13*	36	37
14	196	173
	9 7 1	
-18	126	128
-16	82	132
-15	92	107
-14	194	190
-13	89	80
-12*	41	34
-11*	42	17
-10*	43	61
-9	108	67
-8	351	336
-7*	55	2
-6*	51	127
-5	362	348
-4	88	66
-3*	47	33
-2	156	160
-1	200	238
0	408	352
1	180	174
2*	45	74
3	110	85
4*	42	32
5	413	320
6	357	252
7	103	131
8	91	58
9	158	90
10	319	248
11	131	118
	11 7 1	
-17	129	142
-16	283	321
-15	88	67
-14	67	18
-13*	42	12
-12	103	168
-11	130	104
-10*	42	33
-9	117	427
-7*	41	103
-6*	49	14
-5	132	145
-4*	40	6
-3	429	359
-2	249	214
-1	265	406
0*	48	78
1*	41	14
2*	45	81
3	244	198
4	147	108
5	246	198
6	294	224
7	175	106
8	106	62
	13 7 1	
-14	182	187
-13	88	148
-12	61	102
-11*	49	161
-10*	31	23
-9	101	111
-8	124	124
-7*	35	27
-6	201	207
-5	214	211
-4	147	108
-3	79	44
-2	123	77
-1	242	183
0	519	411
1	150	113
2	66	15
3	80	58
	0 8 1	
-20	125	226
-19	67	17
-18	61	48
-17*	35	76
-16*	39	55
-15	73	77
-14	311	426
-13*	42	89
-12	136	139
-11	89	90
-10	118	124
-9	207	256
-8*	45	87
-7	515	521
-6	505	570
-5	172	226
-4	130	137
-3*	46	76
	2 8 1	
-20	172	263
-19	56	41
-18	88	174
-17*	36	57
-16	132	213
-15*	45	11
-14	297	352
-13	117	237
-12*	44	70
-11*	53	202
-10*	47	111
-9*	46	84
-8*	48	27
-7	322	375
-6	256	314
-5	227	257
-4	364	452
-3	147	216
-2	316	392
-1	100	142
0*	32	67
1*	33	67
2	185	182
3	153	183
4	489	455
5	405	410
6	481	479
7	493	441
8*	44	135
9	167	119
10	351	335
11*	42	24
12	96	120
13	161	196
14	183	221
15	93	96
16	150	163
17*	29	11
18	131	167
	4 8 1	
-20	66	81
-19	58	68
-18	365	477
-17	97	175
-16*	43	36
-15	111	158
-14*	46	21
-13*	42	59
-12	106	132
-11	106	27
-10	115	27
-9	93	87
-8	102	31
-7*	48	5
-6	484	564
-5	191	208
-4	898	856
-3	292	241
-2	207	238
-1*	40	80
0	86	41
1	263	207
2	454	432
3	214	186
4*	48	23
5	136	148
6	228	489
7	121	115
8	407	397
9	100	116
10	343	347
11	167	102
12*	40	26
13	102	77
14	116	98
15	131	146
16	284	352
	6 8 1	
-19	67	17
-18	61	48
-17*	35	76
-16*	39	55
-15	73	77
-14	311	426
-13*	42	89
-12	136	139
-11	89	90
-10	118	124
-9	207	256
-8*	45	87
-7	515	521
-6	505	570
-5	172	226
-4	130	137
-3*	46	76
-2	355	348
-1	183	122
0	104	119
1	98	149
2*	46	28
3	288	219
4	430	315
5	184	135
6	176	137
7	203	215
8	127	137
9	157	118
10	129	127
11	165	188
12*	34	44
13	112	131
14	87	48
	8 8 1	
-19	71	99
-18	203	238
-17	184	233
-16	119	190
-15	198	281
-14	100	43
-13*	38	2
-12	77	45
-11*	48	68
-10	113	38
-9	103	25
-8	118	208
-7	85	59
-6	122	39
-5	142	156
-4	643	624
-3	205	168
-2	90	27
-1	139	59
0	366	324
1	455	391
2	301	260
3	319	255
5	90	75
6	104	37
7	126	102
8	199	141
9	99	109
10	382	356
11	109	66
12	132	110
	10 8 1	
-17*	31	6
-16	120	98
-15*	32	14
-14	158	226
-13	99	93
-12	361	426
-11	107	40
-10	146	113
-9	168	147
-8	176	222
-7	293	308
-6	330	327
-5	154	128
-4	131	114
-3*	43	50
-2	194	177
-1	211	186
0	303	261
1	144	98
2	194	185
3	196	125
4	522	417
5	218	153
6	252	214
7	160	152
8	176	151
	12 8 1	
-14*	28	24
-13	61	27
-12*	30	5
-11	98	115
-10	72	56
-9*	36	92
-8*	37	87
-7*	34	22
-6	123	81
-5	133	124
-4	636	513
-2*	34	52
-1*	33	7
0	144	123
1*	31	73
2	97	65
3	129	70
4	254	205

Table 5. *(Continued)*

l	$\lvert F_o\rvert$	$\lvert F_c\rvert$	l	$\lvert F_o\rvert$	$\lvert F_c\rvert$	l	$\lvert F_o\rvert$	$\lvert F_c\rvert$	l	$\lvert F_o\rvert$	$\lvert F_c\rvert$	l	$\lvert F_o\rvert$	$\lvert F_c\rvert$	l	$\lvert F_o\rvert$	$\lvert F_c\rvert$	l	$\lvert F_o\rvert$	$\lvert F_c\rvert$
1 9 1			5 9 1			-13	393	452	-6	86	144	0*	39	22	-2	170	179	7 11 1			3	294	285
						-12	86	107	-5*	30	32	1	516	467	1	142	136				4	97	88
-18	134	142	-18*	27	107	-11	340	372	-4*	31	70	2	127	88	2	61	43	-14	199	206	5	130	127
-17	72	101	-17*	33	76	-10	118	71	-3*	29	110	3	241	187	3	188	174	-13	82	77	6	59	41
-16	72	130	-16	189	280	-9	104	47	-2*	30	54	5	196	170	4	226	192	-12	125	135	7	123	101
-15	74	101	-15	78	45	-8	90	78	-1	342	381	5	285	239	5	414	413	-11	111	109	8	156	156
-14*	38	70	-14	230	318	-7	184	145	0*	25	29	6	94	17	6	134	108	-10*	36	15	9*	27	43
-13	388	541	-13	401	533	-6	117	69	1	540	605	7	131	138	7	203	168	-9	95	44	10	186	189
-12	101	149	-12*	39	40	-5*	37	6	2*	30	26	8*	33	62	8	393	367	-8	406	399	11	66	66
-11	416	580	-11	333	403	-4	182	140	3	157	159	9	294	283	9	105	100	-7	422	374			
-10	132	178	-10	78	197	-3	149	152	4	121	137	10	67	29	10	205	183	-6*	34	31	4 12 1		
-9	222	303	-9	163	211	-2	279	278	5	226	212	11	79	86	11	126	164	-5*	38	81	-13	183	197
-8*	42	58	-8	114	138	-1	130	76	6	351	326	8 10 1			12	71	86	-4	198	179	-12	348	333
-7	98	86	-7	134	132	0	313	240	7	589	546				13	172	173	-3	436	356	-11	343	265
-6	190	233	-6	135	74	1	489	369	8	191	183	-15	199	181	14	302	276	-2*	34	48	-10	75	3
-5*	38	62	-5*	40	28	2	151	120	9	66	51	-14	81	51				-1*	34	78	-9	222	230
-4	251	311	-4	300	328	3	197	157	10	62	43	-13	155	142	3 11 1			0*	32	28	-8	65	50
-3	153	234	-3*	41	71	4	169	143	11	205	170	-12	60	27	-15	55	69	1*	32	21	-7	207	175
-2	74	110	-2	370	381	5*	37	35	12	149	152	-11*	34	153	-14	204	193	2	110	80	-6	375	385
1	492	448	-1	226	230	6	75	70	13	268	231	-10	114	107	-13*	34	15	3	146	81	-5	88	101
2	59	49	0	294	266	7	116	99	14	144	129	-9	106	121	-12*	31	2	4	132	106	-4	306	259
3	336	311	1	543	457	8	97	91	15	324	288	-8*	33	9	-11	171	192	5	152	126	-3*	26	42
4	197	193	2	108	9							-7	292	311	-10*	34	38	6	356	272	-2*	27	11
5	100	113	3	443	387	11 9 1			4 10 1			-6*	36	43	-9	63	7	7	163	172	-1	72	78
6	169	191	4	336	304	-14*	29	42	-17	72	87	-5	142	153	-8	342	339	8	55	45	0	90	125
7*	42	44	5	303	253	-13	85	116	-16	225	229	-4	299	246	-7	366	352				1	50	41
8	243	265	6	80	41	-12	145	150	-15	173	181	-3	378	306	-6*	34	62	9 11 1			-2	332	305
9*	43	99	7*	42	37	-11*	30	51	-14	66	107	-2	313	302	-5	267	285	-11	83	27	3	98	46
10	74	57	8	203	179	-10	133	151	-13	112	65	-1*	36	40	-4	221	205	-10	248	199	4	158	192
11	343	382	9	200	178	-9	169	196	-12	78	50	0	447	371	-3	415	373	-9	163	148	5*	28	35
12	123	95	10	192	179	-8	98	116	-11	105	73	1	521	427	-2	194	213	-8	287	235	6	354	340
13	183	244	11	237	216	-7	114	88	-10	71	18	2	120	94	-1	245	224	-7	114	72	7	64	44
14	80	64	12	153	172	-6	147	151	-9	326	339	3	239	213	0	70	66	-6	67	103	8	208	183
15	72	12	13	240	275	-5	533	448	-8	112	119	4	144	98	1*	30	21	-5	57	94	9	218	200
16*	32	12	14	60	74	-4	95	51	-7	268	292	5	84	109	2	60	12	-4	273	254	6 12 1		
17*	27	44				-3	180	151	-6	75	77	6	162	137	3	123	136	-3*	32	53			
			7 9 1			-2*	35	4	-5	71	53	7	66	19	4	140	126	-2	279	213	-12*	26	329
3 9 1						-1*	37	60	-4	74	134	8	75	41	5	108	89	-1	83	72	-11	49	42
-18	65	12	-18	70	68	0	188	164	-3	248	240				6	480	414	0	184	140	-10*	26	39
-17	78	16	-17*	31	53	1	73	21	-2	426	441	10 10 1			7	62	82	1*	40	14	-9*	31	51
-16*	33	45	-16*	32	75	2*	36	43	-1	71	106	-13	98	54	8*	34	4	2*	28	6	-8	66	54
-15	65	128	-15	81	57	3	59	44	0	370	364	-12	90	83	9	193	193	3	127	108	-7	103	66
-14	85	95	-14*	38	50	4	87	46	1	128	125	-11	285	276	10*	34	34				-6*	28	6
-13*	38	41	-13	93	150				2	154	163	-10	285	225	11*	30	43	0 12 1			-5	267	250
-12*	41	101	-12	100	98	0 10 1			3	429	383	-9	370	306	12*	27	34	2	116	146	-4	236	214
-11	240	377	-11	88	150				4	152	104	-8	224	200				3	48	69	-3	236	190
-10*	43	81	-10*	42	20	2	328	356	5	104	92	-7	97	69	5 11 1			4	238	241	-2	385	341
-9	136	244	-9	363	483	3	421	422	6	173	180	-6*	32	65				5	133	158	-1	61	60
-8	159	249	-8	93	121	4	92	121	7*	34	11	-5	118	117	-15	146	135	6	348	357	0*	27	51
-7*	41	65	-7	202	235	5*	31	8	8	89	89	-4	137	93	-14	95	76	7	74	33	1	345	301
-6	280	342	-6	158	176	6	178	206	9	223	213	-3	77	84	-13	105	97	8	169	178	2	356	288
-5	392	438	-5	74	36	7	96	134	10*	29	23	-2*	32	11	-12	87	44	9	205	216	3	215	202
-4*	41	35	-4*	41	99	8*	34	30	11	66	18	-1	262	236	-11	98	34	10	139	139	4	52	10
-3	637	638	-3	313	283	9	337	359	12	98	59	0*	36	21	-10*	33	64	11	99	73	5	153	140
-2*	37	9	-2*	41	18	10	128	103	13	113	84	1	219	178	-9	55	17	12	163	153	6*	27	40
-1	190	140	-1	103	111	11	116	91				2	99	103	-8	286	277						
0	150	88	0	112	58	12	64	39	6 10 1			3	259	217	-7	117	77	2 12 1			8 12 1		
1	313	282	1*	41	73	13*	33	33				4	196	148	-6	108	94						
2*	40	16	2	79	51	14	92	73	-16	86	76				-5	109	52	-13	210	221	-9	113	107
3	248	185	3	248	185	15	228	239	-15*	31	64	1 11 1			-4	312	326	-12	257	239	-8	76	45
4	299	264	4	82	49	16*	32	30	-14	141	160				-3*	35	15	-11	55	16	-7	88	60
5	274	269	5	539	456				-13	74	54	-15*	27	77	-2	289	246	-10	212	227	-6	66	71
6	249	276	6	179	153	2 10 1			-12*	35	49	-14	67	95	-1	78	73	-9	70	28	-5*	26	6
7	415	403	7	108	40	-17*	31	24	-11	248	227	-13	89	74	0	426	370	-8*	27	14	-4	340	267
8	87	31	8	177	130	-16*	29	72	-10	75	95	-12*	36	10	1	229	206	-7	54	18	-3*	26	31
9	259	225	9	306	253	-15	60	72	-9	405	369	-11	96	20	2	213	201	-6	73	39	-2	141	151
10	322	327	10	88	11	-14	103	171	-8	327	288	-10	144	147	3*	36	10	-5	207	239	-1	172	161
11	69	19	11	506	492	-13	213	214	-7	364	327	-9	226	238	4	86	48	-4	81	35	0	117	84
12	404	425	12*	29	36	-12*	35	24	-6	121	144	-8	137	157	5	298	276	-3	175	166	1	71	34
13	80	109				-11	555	564	-5	110	134	-7*	33	8	6	302	267	-2	372	345	2	136	116
14	128	180	9 9 1			-10	157	164	-4*	35	15	-6	333	334	7	208	185	-1	175	214			
15	99	11	-16	76	126	-9	95	40	-3	148	167	-5	71	55	8	288	227	0	48	62			
16	225	271	-15*	31	40	-8	192	204	-2	149	157	-4	361	409	9	141	154	1	301	281			
	89	99	-14	234	260	-7	431	433	-1*	35	43	-3	107	144	10	370	303	2	240	228			

Erratum: In Table 5, first page, Column 5, after line 10 from the bottom (hkl = 15 1 3 150 152) heading 0 2 l should be inserted

The superscript is used above to designate a symmetry-equivalent atom. Here and in subsequent discussion the value of this integer corresponds to the order of an atom in the list of equivalent positions presented for space group $C2/c$ in *International tables for x-ray crystallography*, Vol. I. Atoms equivalent by translation other than the C centering of the lattice are not distinguished.

The temperature factors of Table 4 may be seen to be comparable for all atoms of a given specie—*i.e.*, 2.18(4) to 2.67(7) Å^2 for Pb;

2.54(8) Å² for Sb(1), but 1.77(6) to 1.83(2) Å² for Sb(2) through Sb(4), and 1.6(2) to 2.4(4) Å² for the nine sulfur atoms. The observed structure factors are compared in Table 5 with those calculated with the parameters of Table 4.

Discussion of the structure

Interatomic distances along with their estimated standard deviations are summarized for plagionite in Table 6. Bond angles are presented in Tables 7 and 8. Coordination polyhedra for the Pb and Sb atoms are presented in Figs. 2 and 3, while the arrangement of metal atoms about each sulfur atom is depicted in Fig. 4.

Both Pb(2) and Pb(3) display a short apical bond (2.83 and 2.75 Å) above an equatorial plane of four sulfur neighbors which occur at larger distances (2.88—3.07 Å and 2.87—3.04 Å). The locations of these five neighbors are close to five of the six vertices of an octahedral configura-

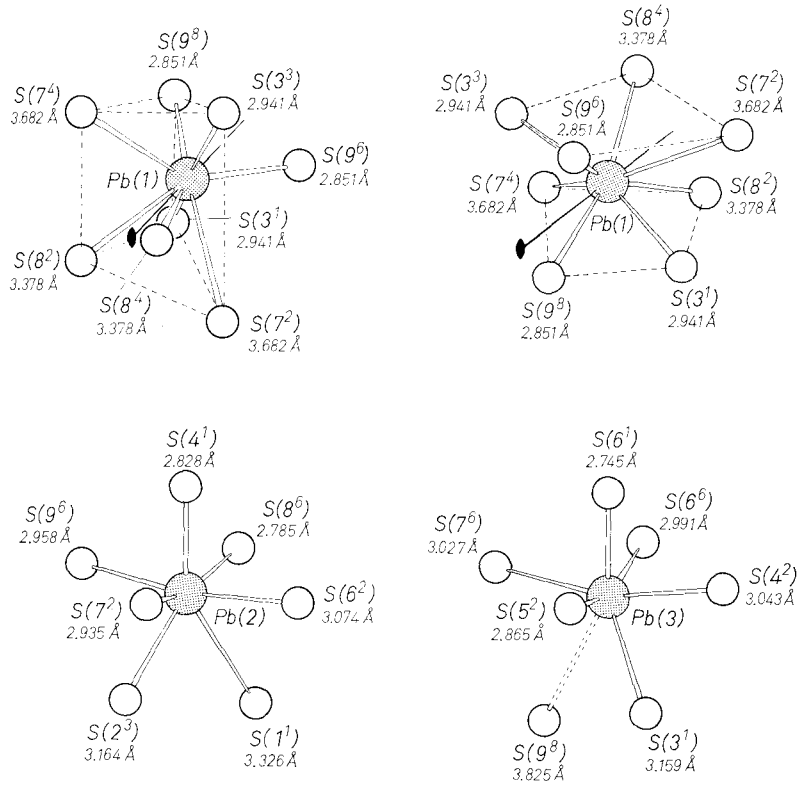

Fig. 2. Polyhedra formed by sulfur atoms about the lead atoms in plagionite

tion. Both Pb atoms have a sixth sulfur atom at still larger distance (3.16 Å) which is displaced from the ideal octahedral location. The average of the bond distances for the six closest sulfur atoms in both the Pb(2) and Pb(3) polyhedra is 2.972 Å, which is virtually identical to the value of 2.965 Å found in the regular octahedron in galena, PbS.

Table 6. *Interatomic distances in plagionite*
(Estimated standard deviations in parentheses. Second-nearest neighbors in brackets)

Pb(1)		Pb(2)		Pb(3)	
S(9^6)	2.851(17) Å (2×)	S(4)	2.828(18) Å	S(6)	2.745(16) Å
S(3)	2.941(14) (2×)	S(8^6)	2.875(15)	S(5^2)	2.865(16)
S(8^2)	3.378(15) (2×)	S(7^2)	2.935(14)	S(6^6)	2.991(14)
[S(7^2)	3.682(16) (2×)]	S(9^6)	2.958(18)	S(7^6)	3.027(16)
		S(6^2)	3.074(15)	S(4^2)	3.043(18)
		S(2^3)	3.164(18)	S(3)	3.159(16)
		S(1)	3.326(15)	[S(9^8)	3.825(18)]
Sb(1)		**Sb(2)**		**Sb(3)**	
S(5)	2.517(17) Å	S(7)	2.436(16) Å	S(8)	2.452(15) Å
S(6^2)	2.677(15)	S(4^2)	2.545(17)	S(2^2)	2.528(18)
S(8^6)	2.685(15)	S(3^2)	2.578(14)	S(3^2)	2.537(14)
S(7^6)	2.924(16)	S(5^6)	3.031(16)	S(5^6)	2.980(17)
S(5^2)	2.969(17)	S(6^6)	3.118(16)	S(4^6)	3.143(17)
[S(2)	3.497(16)]	[S(4)	3.392(18)]	[S(5)	3.555(16)]
[S(1)	3.939(19)]	[S(2^5)	4.141(16)]	[S(3^5)	3.779(15)]
Sb(4)		**S(1)**		**S(2)**	
S(9)	2.440(16) Å	Sb(4^2)	2.488(16) Å (2×)	Sb(4^2)	2.460(18) Å
S(2^2)	2.460(18)	Pb(2)	3.326(15) (2×)	Sb(3^2)	2.528(18)
S(1^2)	2.488(16)	[Sb(1)	3.939(19) (2×)]	Pb(2^3)	3.164(18)
[S(4^6)	3.266(18)]			[Sb(1)	3.497(17)]
[S(6)	3.456(16)]			[Sb(2^5)	4.141(16)]
[S(9^3)	3.720(18)]				
[S(3^6)	3.790(14)]				
S(3)		**S(4)**		**S(5)**	
Sb(3^2)	2.537(14) Å	Sb(2^2)	2.545(17) Å	Sb(1)	2.517(17) Å
Sb(2^2)	2.578(14)	Pb(2)	2.828(18)	Pb(3^2)	2.865(16)
Pb(1)	2.941(14)	Pb(3^2)	3.043(18)	Sb(1^2)	2.969(17)
Pb(3)	3.159(16)	Sb(3^6)	3.143(17)	Sb(3^6)	2.980(17)
[Sb(3^5)	3.779(15)]	[Sb(4^6)	3.266(18)]	Sb(2^6)	3.031(16)
[Sb(4^6)	3.790(14)]	[Sb(2)	3.392(18)]	[Sb(3)	3.555(16)]

Table 6. *(Continued)*

S(6)		S(7)	
$Sb(1^2)$	2.677(15) Å	Sb(2)	2.436(16) Å
Pb(3)	2.745(16)	$Sb(1^6)$	2.924(16)
$Pb(3^6)$	2.991(14)	$Pb(2^2)$	2.935(14)
$Pb(2^2)$	3.074(15)	$Pb(3^6)$	3.027(16)
$Sb(2^6)$	3.118(16)	[$Pb(1^2)$	3.682(16)]
[Sb(4)	3.456(16)]		

S(8)		S(9)	
Sb(3)	2.452(15) Å	Sb(4)	2.440(18) Å
$Sb(1^6)$	2.685(15)	$Pb(1^4)$	2.851(17)
$Pb(2^6)$	2.875(15)	$Pb(2^6)$	2.958(18)
$Pb(1^2)$	3.378(15)	[$Sb(4^3)$	3.720(18)]
		[$Pb(3^8)$	3.827(18)]

Table 7. *Bond angles in the metal-atom coordination polyhedra*
(Estimated standard deviations in parentheses. Bond angles involving one or more second-nearest neighbors are enclosed in brackets. Bond angles involving two of the three shortest bonds for Sb are indicated by an asterisk)

Pb(1)							
$S(8^2)$—Pb(1)—$S(8^4)$	62.5(5)°			$S(3^1)$—Pb(1)—$S(9^6)$	93.6(7)	(2×)	
$S(3^1)$	$S(7^2)$	64.9(4)	(2×)	$S(3^3)$	$S(9^6)$	72.1(4)°	(2×)
$S(7^2)$	$S(8^2)$	66.2(4)	(2×)	$S(7^2)$	$S(8^4)$	72.7(4)	(2×)
$S(8^4)$	$S(3^3)$	71.7(4)	(2×)	$S(7^2)$	$S(9^6)$	83.8(4)	(2×)
				$S(9^6)$	$S(9^8)$	86.1(7)	

Pb(2)			Pb(3)		
$S(1^1)$—Pb(2)—$S(2^3)$	60.7(5)°		[$S(3^1)$—Pb(3)—$S(9^8)$	57.5(4)°]	
$S(1^1)$	$S(6^2)$	70.1(3)	[$S(7^6)$	$S(9^8)$	72.2(4)]
$S(2^3)$	$S(9^6)$	71.8(5)	$S(3^1)$	$S(4^2)$	73.0(4)
$S(4^1)$	$S(7^2)$	77.6(5)	$S(3^1)$	$S(5^2)$	77.4(4)
$S(4^1)$	$S(6^2)$	78.4(4)	$S(5^2)$	$S(6^1)$	78.1(5)
$S(6^2)$	$S(8^6)$	81.3(4)	$S(4^2)$	$S(6^1)$	80.2(5)
$S(4^1)$	$S(8^6)$	83.2(5)	$S(6^1)$	$S(6^6)$	81.0(6)
$S(1^1)$	$S(8^6)$	84.4(4)	$S(6^1)$	$S(7^6)$	82.2(4)
$S(4^1)$	$S(9^6)$	84.8(5)	$S(6^6)$	$S(7^6)$	87.1(4)
$S(6^2)$	$S(7^2)$	87.3(4)	$S(4^2)$	$S(6^6)$	87.2(4)
$S(8^6)$	$S(9^6)$	88.9(4)	$S(5^2)$	$S(7^6)$	87.6(4)
$S(2^3)$	$S(7^2)$	89.0(5)	$S(4^2)$	$S(5^2)$	91.6(5)
$S(7^2)$	$S(9^6)$	96.8(5)	[$S(5^2)$	$S(9^8)$	97.9(4)]
$S(1^1)$	$S(7^2)$	108.0(6)	[$S(6^6)$	$S(9^8)$	99.8(4)]
$S(2^3)$	$S(8^6)$	111.7(4)	$S(3^1)$	$S(6^6)$	122.0(4)
$S(1^1)$	$S(9^6)$	124.9(5)	$S(3^1)$	$S(7^6)$	124.1(4)
$S(2^3)$	$S(6^2)$	126.6(4)	[$S(4^2)$	$S(9^8)$	125.5(4)]

Table 7. *(Continued)*

Sb(1)			Sb(2)		
[S(1^1)—Sb(1)—S(2^1)		52.0(5)°]	[S(2^5)—Sb(2)—S(5^6)		59.8(5)°]
[S(1^1)	S(6^2)	64.4(4)]	[S(2^5)	S(4^1)	64.7(4)]
[S(2^1)	S(5^2)	69.3(5)]	[S(2^5)	S(6^6)	68.3(4)]
[S(1^1)	S(8^6)	75.6(4)]	[S(4^1)	S(4^2)	74.2(5)]
S(5^1)	S(5^2)	79.8(7)	[S(3^2)	S(4^1)	75.0(4)]
S(5^1)	S(7^6)	81.8(5)	S(5^6)	S(7^1)	80.9(5)
[S(2^1)	S(6^2)	83.6(5)	S(5^6)	S(6^6)	81.1(4)
S(5^1)	S(6^2)	85.8(5)*	S(6^6)	S(7^1)	85.4(5)
S(7^6)	S(8^6)	87.0(5)	S(3^2)	S(5^6)	87.2(4)
S(5^2)	S(7^6)	87.7(5)	S(3^2)	S(7^1)	92.0(5)*
S(5^1)	S(8^6)	88.0(5)*	S(4^2)	S(7^1)	92.9(6)*
S(5^2)	S(6^2)	90.1(5)	S(4^2)	S(6^6)	94.1(5)
S(6^2)	S(8^6)	92.7(5)*	S(3^2)	S(4^2)	97.4(5)*
[S(2^1)	S(7^6)	106.9(5)]	[S(2^5)	S(3^2)	106.4(5)]
[S(1^1)	S(5^2)	116.6(5)]	[S(4^1)	S(6^6)	110.3(4)]
[S(2^1)	S(8^6)	123.4(4)]	[S(4^1)	S(5^6)	112.9(5)]
[S(1^1)	S(7^6)	127.3(4)]	[S(2^5)	S(4^2)	123.9(4)]

Sb(3)			Sb(4)		
[S(3^5)—Sb(3)—S(4^6)		63.7(5)°]	[S(3^6)—Sb(4)—S(9^3)		54.0(5)°]
[S(3^5)	S(5^1)	63.9(5)]	[S(3^6)	S(4^6)	65.6(5)]
[S(3^5)	S(5^6)	66.7(4)]	[S(1^2)	S(9^3)	69.1(3)]
[S(2^2)	S(5^1)	72.7(5)]	[S(1^2)	S(6^1)	74.6(6)]
[S(3^2)	S(5^1)	74.5(4)]	[S(9^1)	S(9^3)	75.2(7)]
S(5^6)	S(8^1)	82.9(5)	[S(3^6)	S(9^1)	82.3(5)]
S(4^6)	S(8^1)	84.2(5)	S(1^2)	S(2^2)	83.1(7)*
S(4^6)	S(5^6)	87.6(5)	[S(4^6)	S(9^1)	85.0(5)]
S(3^2)	S(5^6)	89.1(5)	[S(2^2)	S(6^1)	87.7(5)]
S(2^2)	S(8^1)	90.4(6)*	[S(2^2)	S(4^6)	89.7(5)]
S(2^2)	S(4^6)	91.3(5)	[S(6^1)	S(9^3)	93.8(5)]
S(2^2)	S(3^2)	92.1(5)*	[S(3^6)	S(6^1)	95.8(5)]
S(3^2)	S(8^1)	96.4(5)*	S(1^2)	S(9^1)	96.0(5)*
[S(4^6)	S(5^1)	106.0(5)]	S(2^2)	S(9^1)	99.2(6)*
[S(5^1)	S(5^6)	114.0(7)]	[S(4^6)	S(6^1)	105.3(5)]
[S(3^2)	S(3^5)	114.0(5)]	[S(4^6)	S(9^3)	118.0(4)]
[S(2^2)	S(3^5)	118.6(5)]	[S(1^2)	S(3^6)	121.6(5)]

Pb(2) has an additional seventh neighbor S(1) at 3.33 Å which, along with S(2^3), constitute a "split" vertex for the octahedron. The plane defined by this split vertex approximately bisects two of the four equatorial bond angles. This is the case with seven-coordinated Pb atoms in other sulfosalts—*e.g.* aikinite, $PbCuBiS_3$ (I. KOHATSU and

Table 8
Angles between nearest-neighbor bonds in sulfur-atom coordination polyhedra

S(1)					
Pb(2^3)—S(1)—Sb(4^2)	99.5° (2×)		Pb(2^1)—S(1)—Sb(4^2)	111.2° (2×)	
Sb(4^2)	Sb(4^4)	102.0	Pb(2^1)	Pb(2^3)	130.6
S(2)			**S(3)**		
Pb(2^3)—S(2)—Sb(1^1)	89.5°		Pb(1^1)—S(3)—Sb(3^2)	96.2°	
Sb(1^1)	Sb(4^2)	93.6	Sb(2^2)	Sb(3^2)	101.3
Sb(3^2)	Sb(4^2)	103.6	Pb(1^1)	Sb(2^2)	108.0
Pb(2^3)	Sb(4^2)	104.6	Pb(3^1)	Sb(3^2)	112.3
Sb(1^1)	Sb(3^2)	115.1	Pb(3^1)	Sb(2^2)	114.1
Pb(2^3)	Sb(3^2)	141.1	Pb(1^1)	Pb(3^1)	121.8
S(4)			**S(5)**		
Sb(3^6)—S(4)—Sb(4^6)	75.4°		Sb(2^6)—S(5)—Sb(3^6)	82.3°	
Pb(3^2)	Sb(3^6)	85.9	Sb(1^1)	Sb(3^6)	90.2
Pb(2^1)	Sb(4^6)	86.6	Pb(3^2)	Sb(1^2)	91.2
Pb(2^1)	Sb(3^6)	88.9	Sb(1^2)	Sb(2^6)	91.5
Pb(3^2)	Sb(2^2)	92.9	Pb(3^2)	Sb(3^6)	92.3
Pb(2^1)	Sb(2^2)	94.8	Sb(1^1)	Sb(2^6)	96.2
Pb(2^1)	Pb(3^2)	100.1	Pb(3^2)	Sb(1^1)	98.4
Sb(2^2)	Sb(4^6)	105.4	Sb(1^1)	Sb(1^2)	100.2
S(6)			**S(7)**		
Pb(3^6)—S(6)—Sb(2^6)	83.4°		Pb(1^2)—S(7)—Pb(2^2)	80.8°	
Pb(2^2)	Pb(3^6)	88.6	Pb(3^6)	Sb(1^6)	88.9
Pb(2^2)	Sb(1^2)	88.9	Pb(2^2)	Pb(3^6)	90.5
Pb(3^1)	Sb(1^2)	91.6	Pb(1^2)	Sb(2^1)	91.5
Sb(1^2)	Sb(2^6)	95.5	Pb(2^2)	Sb(2^1)	94.6
Pb(3^1)	Sb(1^2)	97.6	Pb(1^2)	Sb(1^6)	96.4
Pb(3^1)	Pb(3^6)	99.0	Pb(3^6)	Sb(2^1)	100.3
Pb(2^2)	Pb(3^1)	101.3	Sb(1^6)	Sb(2^1)	100.8
S(8)			**S(9)**		
Pb(1^2)—S(8)—Sb(3^1)	87.5°		Pb(1^4)—S(9)—Pb(2^6)	96.3°	
Pb(2^6)	Sb(1^6)	93.0	Pb(2^6)	Sb(4^1)	101.4
Sb(1^6)	Sb(3^1)	98.9	Pb(1^4)	Sb(4^1)	101.5
Pb(2^6)	Sb(3^1)	103.3	Pb(1^4)	Pb(3^8)	105.0
Pb(1^2)	Sb(1^6)	109.0	Pb(3^8)	Sb(4^1)	119.9
Pb(1^2)	Pb(2^6)	153.9	Pb(2^6)	Pb(3^8)	127.4

Wuensch, 1971). A seventh sulfur atom may also be located about Pb(3), but it occurs at a significantly larger distance of 3.83 Å, and also falls approximately in the plane defined by S(7^6)—Pb(3)—S(6) rather

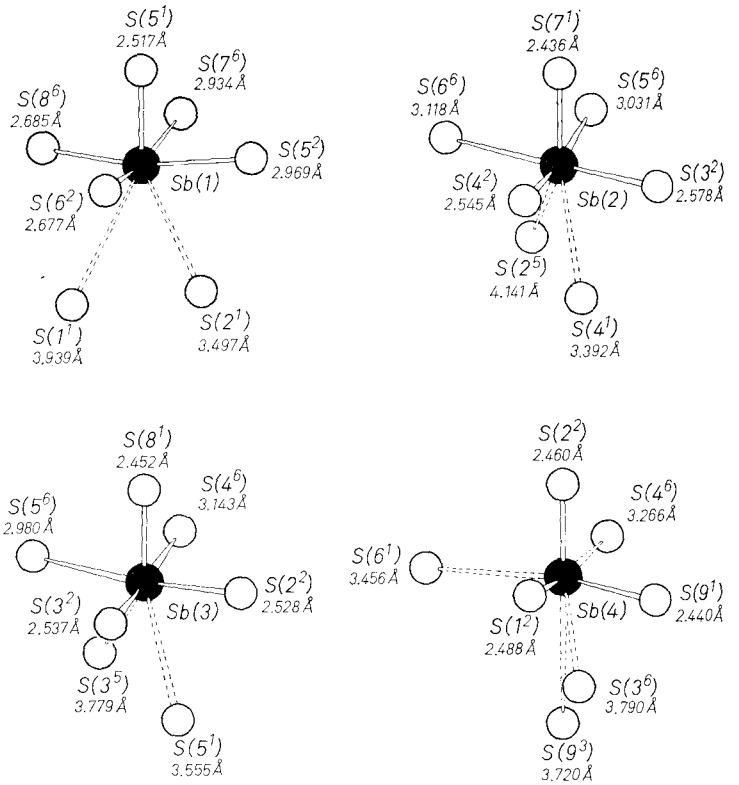

Fig. 3. Polyhedra formed by sulfur atoms about the antimony atoms in plagionite

than bisecting the angle between S(7) and S(6). In subsequent discussion Pb(3) is described as six-coordinated while Pb(2) is considered to have sevenfold coordination. The lead atom which occupies the special position, Pb(1), has markedly different coordination. Six neighbors occur in two symmetry-related and rather separated groups of three at distances of 2.85–3.38 Å (average: 3.06 Å). Seventh and eighth sulfur atom neighbors occur at larger distances of 3.68 Å. This polyhedron may be described as a distorted square antiprism or, alternatively, as a distorted trigonal prism with neighbors along two of the three normals to the prism faces. The latter configuration is more familiar for lead. Both representations are included in Fig. 2.

The sulfur atom arrangement about Sb(1) through Sb(3) displays the [1+2+2] coordination which is frequently found for Sb in sulfosalts. A short apical bond (2.44 to 2.52 Å for the three polyhedra)

Table 9. *Sulfur-sulfur atom separations less than* 5.0 Å *in the metal-atom coordination polyhedra*
(Asterisk indicates contact between a pair of atoms involved in two of the three shortest bonds within a polyhedron)

Pb(1)			Pb(2)		Pb(3)	
$S(3^3)$—$S(9^6)$	3.41 Å	(2×)*	$S(1^1)$—$S(2^3)$	3.28 Å	$S(3^1)$—$S(9^8)$	3.41 Å
$S(3^1)$—$S(7^2)$	3.61	(2×)	$S(2^3)$—$S(9^6)$	3.59	$S(5^2)$—$S(6^1)$	3.54 *
$S(3^3)$—$S(8^4)$	3.72	(2×)	$S(4^1)$—$S(7^2)$	3.61 *	$S(3^1)$—$S(4^2)$	3.69
$S(7^2)$—$S(8^2)$	3.87	(2×)	$S(1^1)$—$S(6^2)$	3.68	$S(6^1)$—$S(6^6)$	3.73 *
$S(9^6)$—$S(9^8)$	3.89		$S(4^1)$—$S(6^2)$	3.73	$S(4^2)$—$S(6^1)$	3.73
$S(7^2)$—$S(8^4)$	4.19	(2×)	$S(4^1)$—$S(8^6)$	3.79 *	$S(3^1)$—$S(5^2)$	3.77
$S(3^1)$—$S(9^6)$	4.22	(2×)	$S(6^2)$—$S(8^6)$	3.88	$S(6^1)$—$S(7^6)$	3.80
$S(7^2)$—$S(9^6)$	4.41	(2×)	$S(4^1)$—$S(9^6)$	3.90	$S(5^2)$—$S(7^6)$	4.08
			$S(8^6)$—$S(9^6)$	4.09	$S(7^6)$—$S(9^8)$	4.09
			$S(6^2)$—$S(7^2)$	4.15	$S(6^6)$—$S(7^6)$	4.15
			$S(1^1)$—$S(8^6)$	4.18	$S(4^2)$—$S(6^6)$	4.16
			$S(2^3)$—$S(7^2)$	4.28	$S(4^2)$—$S(5^2)$	4.24
			$S(7^2)$—$S(9^6)$	4.41		
Sb(1)			Sb(2)		Sb(3)	
$S(1^1)$—$S(2^1)$	3.28 Å		$S(5^6)$—$S(7^1)$	3.58 Å	$S(2^2)$—$S(8^1)$	3.53 Å*
$S(5^1)$—$S(6^2)$	3.54 *		$S(3^2)$—$S(7^1)$	3.61 *	$S(5^6)$—$S(8^1)$	3.62
$S(5^1)$—$S(5^2)$	3.54		$S(4^2)$—$S(7^1)$	3.61 *	$S(2^2)$—$S(3^2)$	3.65 *
$S(5^1)$—$S(7^6)$	3.58		$S(4^1)$—$S(4^2)$	3.65	$S(3^5)$—$S(4^6)$	3.69
$S(5^1)$—$S(8^6)$	3.62 *		$S(3^2)$—$S(4^1)$	3.69	$S(2^2)$—$S(5^1)$	3.70
$S(1^1)$—$S(6^2)$	3.68		$S(2^5)$—$S(5^6)$	3.70	$S(3^2)$—$S(8^1)$	3.72 *
$S(2^1)$—$S(5^2)$	3.70		$S(6^6)$—$S(7^1)$	3.80	$S(3^5)$—$S(5^6)$	3.77
$S(7^6)$—$S(8^6)$	3.87		$S(3^2)$—$S(4^2)$	3.85 *	$S(3^2)$—$S(5^1)$	3.77
$S(6^2)$—$S(8^6)$	3.88 *		$S(5^6)$—$S(6^6)$	4.00	$S(4^6)$—$S(8^1)$	3.79
$S(5^2)$—$S(6^2)$	4.00		$S(2^5)$—$S(4^1)$	4.08	$S(3^2)$—$S(5^6)$	3.88
$S(5^2)$—$S(7^6)$	4.08		$S(2^5)$—$S(6^6)$	4.16	$S(3^5)$—$S(5^1)$	3.88
$S(2^1)$—$S(6^2)$	4.16		$S(4^2)$—$S(6^6)$	4.16	$S(2^2)$—$S(4^6)$	4.08
$S(1^1)$—$S(8^6)$	4.18				$S(4^6)$—$S(5^6)$	4.24
Sb(4)						
$S(1^2)$—$S(2^2)$	3.28 Å*		$S(1^2)$—$S(6^1)$	3.68 Å	$S(4^6)$—$S(9^1)$	3.90 Å
$S(3^6)$—$S(9^3)$	3.41		$S(2^2)$—$S(9^1)$	3.73 *	$S(2^2)$—$S(4^6)$	4.08
$S(1^2)$—$S(9^1)$	3.66 *		$S(3^6)$—$S(4^6)$	3.85	$S(2^2)$—$S(6^1)$	4.16
$S(1^2)$—$S(9^3)$	3.66		$S(9^1)$—$S(9^3)$	3.89	$S(3^6)$—$S(9^1)$	4.22

occurs to a sulfur atom situated above an equatorial plane comprised of neighbors at two approximately equal intermediate distances [2.53 Å for Sb(3)—$S(2^2)$ to 2.69 Å for Sb(1)—$S(8^6)$]. Fourth and fifth neighbors occur at still larger and approximately equal distances of 2.92 Å

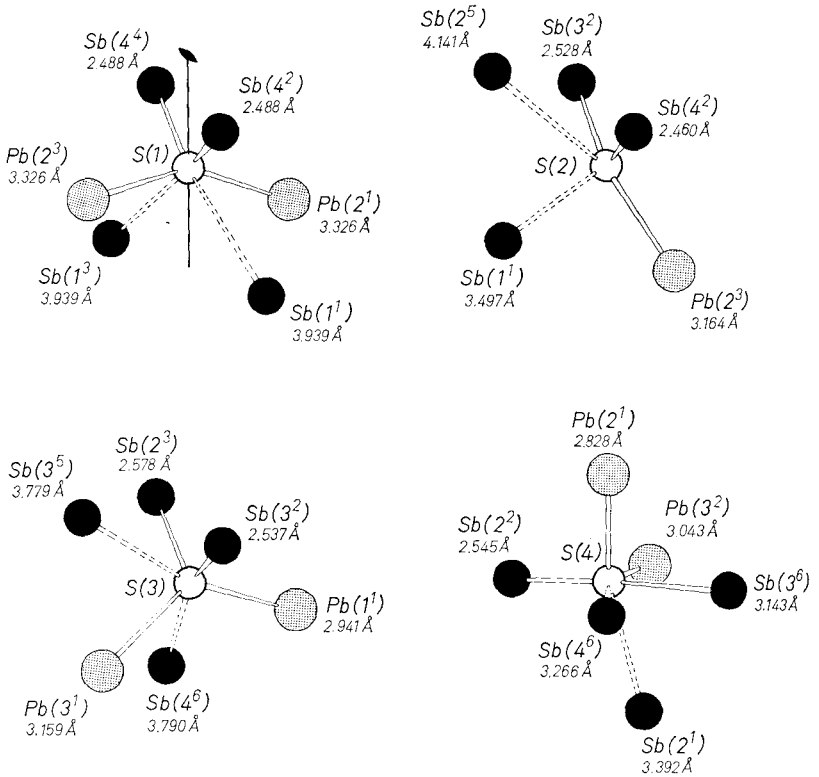

Fig. 4/1

Fig. 4. Polyhedra formed by the metal atoms about the sulfur atoms in plagionite

[Sb(1)—S(7⁶)] to 3.14 Å [Sb(3)—S(4⁶)]. Averages for the three sets of distances in the three coordination polyhedra of this type in plagionite are 2.468, 2.592 and 3.028 Å. The fourth antimony atom, Sb(4), displays a slightly different coordination scheme: The first three neighbors are at comparable lengths, while the fourth and fifth neighbors occur at distances which are larger than those of corresponding neighbors in the five-coordinated groups. Sb(4) is therefore described as 3-coordinated in subsequent discussion. The simultaneous occurrance of [3] and [1+2+2] coordinated groups is not unknown in Sb sulfides. A notable example is stibnite, Sb_2S_3 (ŠĆAVNIČAR, 1960; BAYLISS and NOWACKI, 1972). Sixth and seventh S neighbors may be located about each of the four independent Sb atoms, but these occur at much larger distances of 3.39 Å [Sb(2)—S(4)] to 4.14 Å [Sb(2)—S(2⁵)]. Sulfur-atom

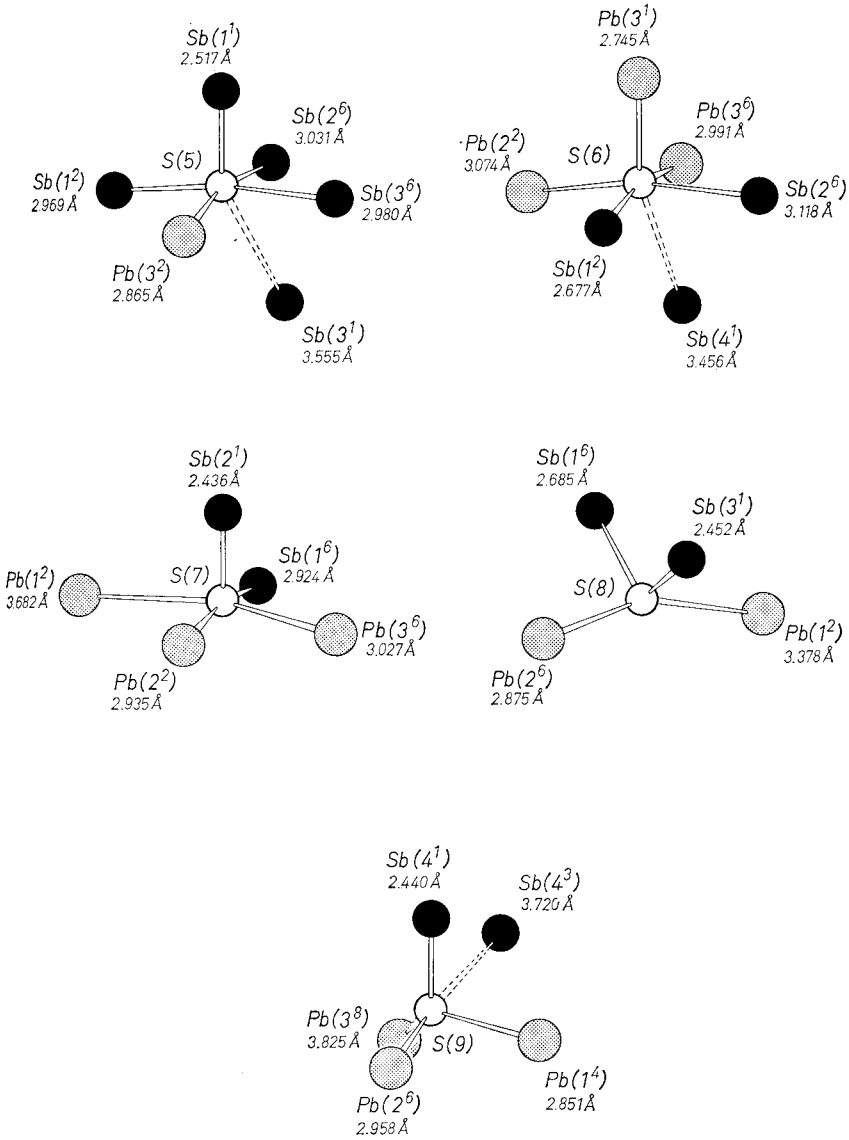

Fig. 4/2

contact distances in the metal-atom coordination polyhedra are summarized in Table 9. Few distances are less than the van der Waals contact distance of 3.70 Å. The primary exceptions are contacts

between the sulfur atoms involved in the shortest bonds to the metal atoms.

On the basis of the nearest and next-nearest neighbor configuration which has somewhat arbitrarily been assigned to the metal-atom coordination, the sulfur-atom polyhedra fall into three groups: 3-coordinated [S(2) and S(9)], distorted tetrahedral coordination by two Sb and two Pb atoms [S(1), S(3) and S(8)] and fivefold square-pyramidal coordination [S(4), S(5), S(6) and S(7)]. The sulfur-atom polyhedra are depicted in Fig. 4. It is of interest to note that, in the five-coordinated polyhedra present in the structure, the metal atoms are invariably displaced *downward* from the base of the square pyramid (*i.e.*, away from the apical sulfur atom), while the five-coordinated sulfur atoms are displaced *upwards*.

A projection of the plagionite structure along b is presented in Fig. 5. The most immediately noticed feature of the structure is the grouping of metal and sulfur atoms on alternate (400) planes. In particular, a cluster of two Pb(2) and two Pb(3) pseudo-octahedra share edges to form a four-membered string parallel to c. These clusters are linked by the Pb(1) polyhedra to form a continuous chain of Pb groups in (010) which runs parallel to $[10\bar{1}]$. The Pb chain is flanked by Sb square pyramids which share an apical edge with the Pb octahedra. The bases of the Sb square pyramids, and also the equatorial plane of the Pb octahedra, are oriented parallel to $\{112\}$. Two-layer slabs parallel to (112) and $(1\bar{1}2)$, respectively, alternate along c. The boundaries of these PbS-like regions are (002) planes which pass through the twofold axes of the structure at $z = 1/4$ and $3/4$. Equivalent PbS-like slabs are repeated by b within these domains. The irregularly-coordinated Pb atom [Pb(1)] as well as the Sb atom and the S atoms with low coordination numbers may be seen to occur at the (002) boundaries of the rocksalt-like units. The pseudo-octahedral polyhedra occur within the interior of the rocksalt slabs of the structure.

All Pb-Sb sulfosalts other than members of the plagionite group would appear to be based upon stibnite-like chains (*i.e.*, a rocksalt-like slab which is two atoms in thickness) by virtue of their displaying one lattice constant equal to a multiple of 4 Å. The members of the plagionite group do not display this periodicity nor do they possess acicular habits with axes of elongation parallel to such a translation. It is therefore of great interest to note that the structure of plagionite may also be described in terms of similar infinite ribbons. The structure is merely such that the ribbons extend parallel to $\langle 110 \rangle$ rather than one

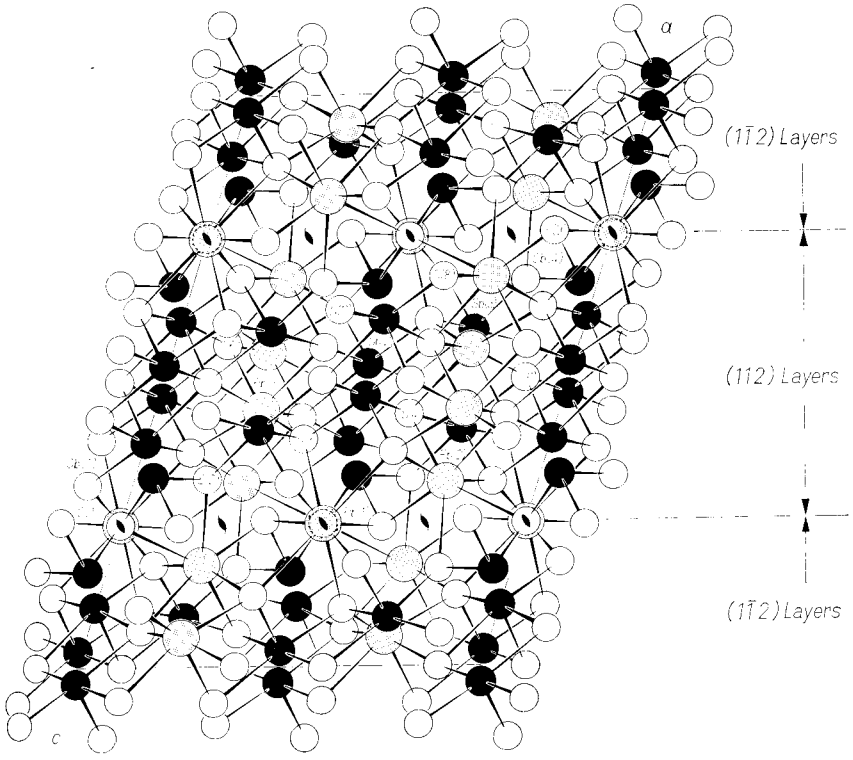

Fig. 5. Projection of the structure of plagionite along b

of the cell edges. Traced in (010) the structure may be seen to consist of twisted ribbons of rocksalt-like slabs running parallel to (112) and (1$\bar{1}$2). The lead atom [Pb(1)] and sulfur atom [S(1)] in special positions act as pivot points common to {112} slabs which are related by a two-fold rotation.

The rocksalt-like nature of the structure is best appreciated in a projection of the structure on (112). Figure 6 presents this projection; only atoms within *ca.* 7 to 11 Å above the origin of the cell are depicted [the first (112) rocksalt unit to be encountered in the cell upon moving out from the origin along c]. In this projection the rocksalt regions may be readily seen to extend indefinitely along [$\bar{1}$10]. Unlike the (presumably) stibnite-related Pb-Sb sulfosalts, the direction of extension of the ribbon is $[130]_{PbS}$ rather than $[110]_{PbS}$. The basis for selection of the asymmetric unit is displayed in the (112) projection. The designated

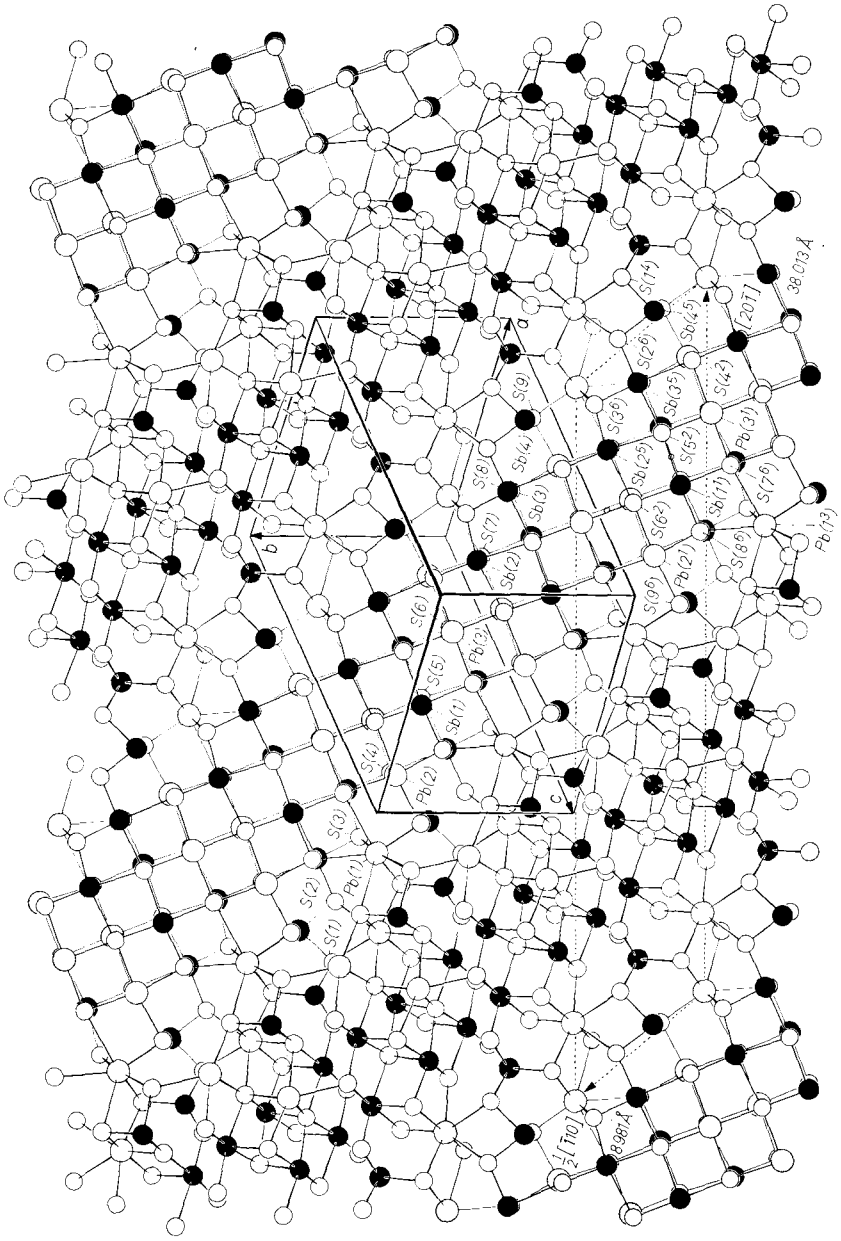

Fig. 6. Projection of a limited portion of the plagionite structure (from *ca.* 7 to 11 Å above the origin of the cell) onto (112), the cleavage plane of the structure. The periodicity of the projection may be defined in terms of the dotted net given by $\frac{1}{2}[\bar{1}10]$, 8.981 Å, and [20$\bar{1}$], 38.013 Å, both of which lie in (112). Elevations above the origin of the atoms designated within the net are summarized in Table 10

asymmetric unit consists of a single chain of metal-sulfur pairs which extends along $[110]_{PbS}$.

The bonds within the PbS-like region are close to being orthogonal in the interior of the region. Distortion occurs near the boundaries. This is perhaps a result of accumulated misfit between Pb and Sb groups, but in part occurs because atoms belong to adjacent (112) and $(1\bar{1}2)$ layers. The reason for the distinct coordinations of Pb(1) and Sb(4) is apparent in Fig. 6. Four of the eight bonds about Pb(1) represent distortions of semi-orthogonal rocksalt-like bonds in neighboring {112} slabs. Similarly, the $Sb(4)S_3$ group is linked to an equivalent group in $(1\bar{1}2)$ by twofold rotation about S(1). In order to maintain the Sb(4)—S(1) bond the antimony atom pulls away from the rocksalt-like region. The rocksalt-like layer is not only close in orientation to (112), but is remarkably planar. Table 10 summarizes the elevation, above the origin, of the atoms in the upper layer of Fig. 6. [The lower layer is equivalent and is related by inversion centers which occur between layers at locations indicated in Fig. 6 by the small circles to the right of $Sb(1^1)$ and above $S(6^2)$.] The root-mean-square departure from the mean elevation amounts to only 0.219 Å.

The manner in which neighboring (112) rocksalt-like layers interface upon repetition by b is illustrated in Fig. 7. The diagram is again a projection onto (112) and presents the lower layer of atoms in the

Table 10. *Elevation of the asymmetric unit above the origin of the cell of plagionite, measured in a direction normal to* (112)

(Designated atoms are identified in Fig. 6. Variations in averages are root-mean-square deviations from mean)

Atom	Elevation	Atom	Elevation
$Pb(1^3)$	9.883 Å	$S(1^4)$	10.335 Å
$Pb(2^1)$	10.300	$S(2^6)$	10.254
$Pb(3^1)$	10.473	$S(3^6)$	10.407
$Sb(1^1)$	10.182	$S(4^2)$	10.162
$Sb(2^5)$	10.226	$S(5^2)$	9.968
$Sb(3^5)$	10.283	$S(6^2)$	9.911
$Sb(4^5)$	10.263	$S(7^6)$	9.850
		$S(8^6)$	9.812
		$S(9^6)$	9.787
Average for metal atoms	10.230 ± 0.165	Average for sulfur atoms	10.054 ± 0.225
Average for all atoms	10.131 ± 0.219		

PbS-like region of Fig. 6 plus the upper layer of atoms in the adjacent slab (equivalent to the upper layer of atoms in Fig. 6 by the b translation). The shorter of the two "split vertex" bonds of the Pb and Sb atoms in pseudo-octahedral coordination may be seen to function as weak bonds between the rocksalt-like layers. The shift between neighboring layers is approximately $\frac{1}{2}[100]_{PbS}$, and the interface between adjacent two-layer slabs may thus be regarded as a weak, distorted continuation of rocksalt-like structure.

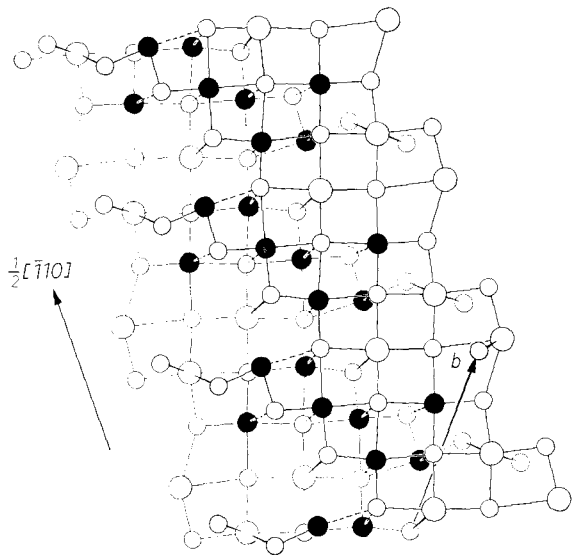

Fig. 7. Projection onto (112) of an interface between adjacent rocksalt-like layers in the plagionite structure

The presence of weakly-bonded interfaces between rocksalt-like slabs of atoms parallel to {112} explains nicely the {112} cleavage which is observed in the plagionite group. The composition of the series, $Pb_{3+2n}Sb_8S_{15+n}$, may be accounted for in terms of the addition of one Pb and one S atom to the asymmetric unit of neighboring members. The uniform increase in c throughout the series may be explained if the additional Pb and S atoms serve to increase the length of the chain-like asymmetric unit and hence the width of the rocksalt-like ribbon of Fig. 6. The extent of the overlap of weakly-bonded {112} layers (Fig. 7) would increase as the number of Pb atoms in the layer

increased. This feature would account for the observed increase in perfection of the {112} cleavage as one procedes through the series.

A recent determination of the structure of semseyite in this laboratory (J. KOHATSU, 1973; J. KOHATSU and WUENSCH, 1974a) has confirmed this proposed relation between the structures. On the basis of a comparison between semseyite and plagionite, it has been possible to predict structures for the remaining known members of the plagionite group (fülöppite, $Pb_3Sb_8S_{15}$, and heteromorphite, $Pb_7Sb_8S_{19}$) as well as to predict structures for hypothetical additional members of the homologous series (J. KOHATSU, 1973; J. KOHATSU and WUENSCH, 1974b).

Acknowledgements

The writers are indebted to Professor C. FRONDEL, who provided the crystals employed in this study and to Dr. JUDITH JENKINS KOHATSU for helpful discussion of the structure. The study was supported by Grants GA-1549 and GA-22698 from the Earth Sciences Section of the National Science Foundation.

References

PETER BAYLISS and WERNER NOWACKI (1972), Refinement of the crystal structure of stibnite, Sb_2S_3. Z. Kristallogr. **135**, 308—315.

L. BORN and E. HELLNER (1960), A structural proposal for boulangerite. Amer. Mineral. **45**, 1266—1271.

M. J. BUERGER (1937), The precision determination of the linear and angular lattice constants of single crystals. Z. Kristallogr. **97**, 433—468.

CHARLES W. BURNHAM (1962), Lattice constant refinement. Carnegie Inst. Washington Year Book **61**, 133—135.

SEUNG-AM CHO and B. J. WUENSCH (1970), Crystal chemistry of the plagionite group. Nature [London] **225**, 444—445.

E. B. FLEISCHER, R. B. K. DEWAR and A. L. STONE (1967), Use of the symbolic addition method in the solution of centrosymmetric structures; description of a computer program to automate the process. Abstract A 7, Program and Abstracts, Winter Meeting of the Amer. Crystallogr. Assoc., 20.

J. L. JAMBOR (1969), Sulphosalts of the plagionite group. Miner. Mag. **37**, 442—446.

IWAO KOHATSU and B. J. WUENSCH (1971), The crystal structure of aikinite, $PbCuBiS_3$. Acta Crystallogr. B **27**, 1245—1252.

JUDITH JENKINS KOHATSU (1973), The crystal chemistry of the homologous series $Pb_{3+2n}Sb_8S_{15+2n}$ (the plagionite group). Ph.D. Thesis, Department of Metallurgy and Materials Science, Massachusetts Institute of Technology.

JUDITH JENKINS KOHATSU and B. J. WUENSCH (1974*a*), The crystal structure of semseyite, $Pb_9Sb_8S_{21}$, the final known member in the homologous series $Pb_{3+2n}Sb_8S_{15+2n}$. Acta Crystallogr. [in press].

JUDITH JENKINS KOHATSU and B. J. WUENSCH (1974*b*), The crystal chemistry of the homologous series $Pb_{3+2n}Sb_8S_{15+2n}$ and predicted structures for $Pb_3Sb_8S_{15}$ (fülöppite) and $Pb_7Sb_8S_{19}$ (heteromorphite). Acta Crystallogr. [to be published].

WERNER NOWACKI (1969), Zur Klassifikation und Kristallchemie der Sulfosalze. Schweiz. Miner. Petrogr. Mitt. **49**, 109–156.

E. W. NUFFIELD (1946), Studies of mineral sulpho-salts: XII—Fülöppite and zinckenite. Univ. Toronto Studies, Geol. Ser. **50**, 49–62.

E. W. NUFFIELD and M. A. PEACOCK (1945), Studies of mineral sulpho-salts: VIII—Plagionite and semseyite. Univ. Toronto Studies, Geol. Ser. **49**, 17–39.

HAJO H. ONKEN (1964), Manual for some computer programs for x-ray analysis. Crystallographic Laboratory, M.I.T., Cambridge, Massachusetts.

CHARLES PALACHE, HARRY BERMAN and CLIFFORD FRONDEL (1944), *The system of mineralogy*, Vol. I, seventh edition. John Wiley and Sons, New York, 464.

CHARLES T. PREWITT (1962), Structures and crystal chemistry of wollastonite and pectolite. Ph.D. Thesis, Department of Geology and Geophysics, Massachusetts Institute of Technology.

S. ŠĆAVNIČAR (1960), The crystal structure of stibnite. A redetermination of atomic positions. Z. Kristallogr. **114**, 85–97.

HIROSHI TAKEDA and HIROYUKI HORIUCHI (1971), Symbolic addition procedure applied to zinckenite structure determination. Miner. J. Japan **9**, 283–295, [in Japanese].

BERNHARDT J. WUENSCH (1972), The crystal chemistry of sulfur. Section 16A in *Handbook of Geochemistry*, Vol. II/3. Springer Verlag, Berlin.